Atmospheric
Chemistry
and Physics

The impact of chlorine chemistry combined with heterogeneous N_2O_5 reactions on air quality in China

Xiajie Yang[1,2], **Qiaoqiao Wang**[1,2], **Nan Ma**[1,2], **Weiwei Hu**[3], **Yang Gao**[4], **Zhijiong Huang**[1,2], **Junyu Zheng**[1,2], **Bin Yuan**[1,2], **Ning Yang**[1,2], **Jiangchuan Tao**[1,2], **Juan Hong**[1,2], **Yafang Cheng**[5], and **Hang Su**[5]

[1]Institute for Environmental and Climate Research, Jinan University, Guangzhou 511443, China
[2]Guangdong–Hongkong–Macau Joint Laboratory of Collaborative Innovation for Environmental Quality,
Guangzhou 511443, China
[3]Guangzhou Institute of Geochemistry, Chinese Academy of Sciences, Guangzhou 510640, China
[4]Key Laboratory of Marine Environment and Ecology, Ministry of Education,
Ocean University of China, Qingdao 266100, China
[5]Max Planck Institute for Chemistry, Mainz 55128, Germany

Correspondence: Qiaoqiao Wang (qwang@jnu.edu.cn)

Abstract. The heterogeneous reaction of N_2O_5 on Cl-containing aerosols (heterogeneous $N_2O_5 + Cl$ chemistry) plays a key role in chlorine activation, NO_x recycling, and consequently O_3 and $PM_{2.5}$ formation. In this study, we use the GEOS-Chem model with additional anthropogenic and biomass burning chlorine emissions combined with updated parameterizations for the heterogeneous $N_2O_5 + Cl$ chemistry (i.e., the uptake coefficient of N_2O_5 ($\gamma_{N_2O_5}$) and the $ClNO_2$ yield (φ_{ClNO_2})) to investigate the impacts of chlorine chemistry on air quality in China, the role of the heterogeneous $N_2O_5 + Cl$ chemistry, and the sensitivity of air pollution formation to chlorine emissions and parameterizations for $\gamma_{N_2O_5}$ and φ_{ClNO_2}. The model simulations are evaluated against multiple observational datasets across China and show significant improvement in reproducing observations of particulate chloride, N_2O_5, and $ClNO_2$ when including anthropogenic chlorine emissions and updates to the parameterization of the heterogeneous $N_2O_5 + Cl$ chemistry relative to the default model. The simulations show that total tropospheric chlorine chemistry could increase annual mean maximum daily 8 h average (MDA8) O_3 by up to 4.5 ppbv but decrease $PM_{2.5}$ by up to 7.9 µg m^{-3} in China, 83 % and 90 % of which could be attributed to the effect of the heterogeneous $N_2O_5 + Cl$ chemistry. The heterogeneous uptake of N_2O_5 on chloride-containing aerosol surfaces is an important loss pathway of N_2O_5 as well as an important source of O_3 and hence is particularly useful in elucidating the commonly seen ozone underestimations relative to observations. The importance of chlorine chemistry largely depends on both chlorine emissions and the parameterizations for the heterogeneous $N_2O_5 + Cl$ chemistry. With the additional chlorine emissions, the simulations show that annual MDA8 O_3 in China could be increased by up to 3.5 ppbv. The corresponding effect on $PM_{2.5}$ concentrations varies largely with regions, with an increase of up to 4.5 µg m^{-3} in the North China Plain but a decrease of up to 3.7 µg m^{-3} in the Sichuan Basin. On the other hand, even with the same chlorine emissions, the effects on MDA8 O_3 and $PM_{2.5}$ in China could differ by 48 % and 27 %, respectively, between different parameterizations.

1 Introduction

Chlorine (Cl) plays an important role in atmospheric chemistry in both the stratosphere and the troposphere, primarily via the reactions of the Cl atom with various atmospheric trace gases including dimethyl sulfide, methane, and other volatile organic compounds (VOCs). The chemistry of Cl is quite similar with that of hydroxyl radicals (OH) while Cl atoms react up to 2 orders of magnitude faster with some VOCs than OH (Atkinson et al., 2006). Studies have shown that Cl accounts for around 2.5 %–2.7 % of the global CH_4 oxidation in the troposphere, and the contribution varies across regions, reaching up to 10 %–15 % in Cabo Verde and $\sim 20\%$ in east China (Lawler et al., 2011; Hossaini et al., 2016). The Cl atom, therefore, is regarded as a potentially important tropospheric oxidant.

In general, Cl atoms can be produced from the photodissociation and the oxidation of chlorinated organic species (e.g., CH_3Cl, CH_2Cl_2, and $CHCl_3$) and inorganic chlorine species (i.e., HCl and Cl_2) (Saiz-Lopez and Von Glasow, 2012; Simpson et al., 2015). Nitryl chloride ($ClNO_2$), formed through the heterogeneous reaction between dinitrogen pentoxide (N_2O_5) and chloride-containing aerosols (hereinafter referred to as the heterogeneous $N_2O_5 + Cl$ chemistry), is found to be another important source of tropospheric Cl atoms in polluted regions (Liu et al., 2018; Haskins et al., 2019; Choi et al., 2020; Simpson et al., 2015). The heterogeneous formation of $ClNO_2$ and the subsequent photolysis can be described by Reactions (R1)–(R4) shown below (Finlayson-Pitts et al., 1989; Osthoff et al., 2008). The net Reactions (R1) (N_2O_5 hydrolysis on non-chloride-containing aerosols) and (R2) (uptake of N_2O_5 on chloride-containing aerosols) could be expressed as Reaction (R3), in which the $ClNO_2$ yield (i.e., φ_{ClNO_2}, defined as the molar ratio of produced $ClNO_2$ to total reacted N_2O_5) represents the fraction of N_2O_5 reacting via Reaction (R2).

$$N_2O_5(g) + H_2O(aq) \rightarrow 2\,HNO_3(aq) \tag{R1}$$

$$N_2O_5(g) + HCl(aq) \rightarrow HNO_3(aq) + ClNO_2(g) \tag{R2}$$

$$N_2O_5(g) + (1-\varphi)H_2O(aq) + \varphi HCl(aq)$$
$$\rightarrow (2-\varphi)HNO_3(aq) + \varphi ClNO_2(g) \tag{R3}$$

$$ClNO_2(g) + h\nu \rightarrow Cl(g) + NO_2(g) \tag{R4}$$
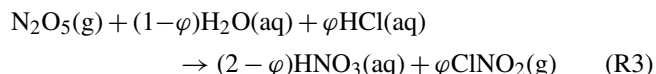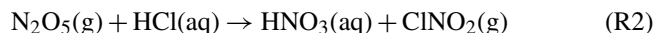
Estimates based on model simulations have suggested that $ClNO_2$ provides a source of Cl atoms totaling $0.66\,Tg\,Cl\,a^{-1}$, with the vast majority (95 %) being in the Northern Hemisphere (Sherwen et al., 2016). The relative contribution of $ClNO_2$ to global tropospheric Cl atoms is 14 % on average and exhibits clear regional variations (Sherwen et al., 2016). For example, the study by Riedel et al. (2012) reported that the relative contribution is approximately 45 % in Los Angeles based on a simple box model combined with local observations.

The heterogeneous formation of $ClNO_2$ also serves as a reservoir for reactive nitrogen at night. The rapid photolysis of $ClNO_2$ at daytime (Reaction R4) not only releases highly reactive Cl atoms but also recycles NO_2 back to the atmosphere, which also significantly affects the daytime photochemistry (Riedel et al., 2014). Previous global and hemispheric models found that the heterogeneous $N_2O_5 + Cl$ chemistry could increase monthly mean values of the maximum daily 8 h average (MDA8) O_3 concentrations by 1.0–8.0 ppbv in most Northern Hemisphere regions (Sarwar et al., 2014; Wang et al., 2019). The reaction also impacts secondary aerosol formation, mainly through the recycling of NO_x (Staudt et al., 2019; Mitroo et al., 2019). For example, Sarwar et al. (2014) estimated that $ClNO_2$ production decreases nitrate by 3.3 % in winter and 0.3 % in summer averaged over the entire Northern Hemisphere. The influence of the heterogeneous formation of $ClNO_2$ in China is even larger due to the polluted environment, leading to an increase in ozone concentrations by up to 7 ppbv and a decrease in total nitrate by up to $2.35\,\mu g\,m^{-3}$ on a monthly mean basis (Li et al., 2016; Sarwar et al., 2014)

There are two key parameters that determine the uptake efficiency of N_2O_5 and production of $ClNO_2$, the aerosol uptake coefficient of N_2O_5 ($\gamma_{N_2O_5}$) and the $ClNO_2$ yield (φ_{ClNO_2}). The most widely used parameterization for $\gamma_{N_2O_5}$ and φ_{ClNO_2} was proposed by Bertram and Thornton (2009) (hereinafter referred to as BT09), which is based on the laboratory studies with considerations of aerosol water content, concentrations of nitrate and chloride, and specific surface area (i.e., the ratio of surface area concentrations to particle volume concentrations). However, recent field and model studies have shown that this parameterization would overestimate both $\gamma_{N_2O_5}$ and φ_{ClNO_2}, especially in regions with high Cl levels (Mcduffie et al., 2018b, a; Xia et al., 2019; Chang et al., 2016; Hong et al., 2020; Yu et al., 2020). The discrepancies could be partly attributed to the complexity of atmospheric aerosols (e.g., mixing state and complex coating materials) in contrast to the simple proxies used in laboratory studies (Yu et al., 2020). Specifically, the suppressive effect of organic coatings is not considered in BT09. Several parameterizations updated from BT09 have been proposed by more recent studies based on field measurements and box model studies (Yu et al., 2020; Mcduffie et al., 2018a, b; Xia et al., 2019). However, some of these previous field-based parameterizations were derived from observations under different ambient conditions which may not be applicable to the highly polluted regions in China. A full evaluation of the representativeness of different parameterizations for the heterogeneous $N_2O_5 + Cl$ chemistry and the associated impacts on ambient air quality in China is not available yet.

In addition to the parameterization, the influence of the heterogeneous $N_2O_5 + Cl$ chemistry is also sensitive to chlorine emissions. In early modeling studies, global tropospheric chlorine is mainly from sea salt aerosols (SSA), and most of the chlorine over continental regions in North America and Europe is dominated by the long-range transport of SSA (Wang et al., 2019; Sherwen et al., 2017). The study by

Wang et al. (2019) found an addition of anthropogenic chlorine emissions in the model would result in overestimates of HCl observations in the US and suggested insignificant influence of anthropogenic Cl in the US. However, there are also studies pointing out the importance of anthropogenic chlorine emissions in China (Le Breton et al., 2018; Yang et al., 2018; Hong et al., 2020). The study by X. Wang et al. (2020) suggested that anthropogenic chlorine emissions in China are more than 8 times higher than those in the US and could dominate reactive chlorine in China, resulting in an increase in $PM_{2.5}$ and ozone by up to $3.2\,\mu g\,m^{-3}$ and $1.9\,ppbv$ on an annual mean basis, respectively. The comprehensive effects of anthropogenic chlorine on air quality as well as their sensitivities to different parameterizations for the heterogeneous $N_2O_5 + Cl$ chemistry, however, has not been investigated in previous studies.

In this work, we use the GEOS-Chem model to investigate the impacts of chlorine chemistry including the heterogeneous $N_2O_5 + Cl$ chemistry on air quality in China. Multiple observational datasets, including N_2O_5, $ClNO_2$, O_3, $PM_{2.5}$, and its chemical compositions from different representative sites across China, are used to assess the model performance. With comprehensive chlorine emissions as well as appropriate parameterizations for the heterogeneous $N_2O_5 + Cl$ chemistry, our objectives are (1) to improve the model's performance regarding the simulation of particulate chloride, $ClNO_2$, N_2O_5, $PM_{2.5}$, and O_3 concentrations and (2) to extend the investigation on the effects of chlorine chemistry on both $PM_{2.5}$ and ozone pollution in China as well as their sensitivities to anthropogenic chlorine emissions and the parameterizations for the heterogeneous $N_2O_5 + Cl$ chemistry.

2 Methodology

2.1 GEOS-Chem model

The GEOS-Chem model (version 12.9.3, http://www.geos-chem.org, last access: 14 March 2022, https://doi.org/10.5281/zenodo.3974569) is driven by assimilated meteorological fields (GEOS-FP) from the NASA Global Modeling and Assimilation Office (GMAO) at NASA Goddard Space Flight Center. The simulation in this study was conducted in a nested-grid model with a native horizontal resolution of $0.25° \times 0.3125°$ (latitude × longitude) and 47 vertical levels over East Asia ($15°\,S–55°\,N$, $70–140°\,E$). The dynamical boundary conditions were from a global simulation with a horizontal resolution of $2° \times 2.5°$. We initialized the model with a 1 month spinup followed by a 1-year simulation for 2018. The simulation included a detailed representation of coupled NO_x–ozone–VOC–aerosol–halogen chemistry (Sherwen et al., 2016; Wang et al., 2019). Previous studies have demonstrated the ability of GEOS-Chem to reasonably reproduce the magnitude and seasonal variation in surface ozone and particulate matter

over east Asia and China (Wang et al., 2013; Geng et al., 2015; Li et al., 2019).

2.1.1 Chlorine chemistry

The GEOS-Chem model includes a comprehensive chlorine chemistry mechanism coupled with bromine and iodine chemistry. Full details could be found in the study of Wang et al. (2019). Briefly, the model includes 12 gas-phase inorganic chlorine species (Cl, Cl_2, Cl_2O_2, $ClNO_2$, $ClNO_3$, ClO, ClOO, OClO, BrCl, ICl, HOCl, HCl), three gas-phase organic chlorine species (CH_3Cl, CH_2Cl_2, $CHCl_3$), and aerosol Cl^- in two size bins (fine mode with radius $\leq 0.5\,\mu m$ and coarse mode with radius $> 0.5\,\mu m$). The gas–aerosol equilibrium between HCl and Cl^- is calculated with ISORROPIA II (Fountoukis and Nenes, 2007) as part of the H_2SO_4–HCl–HNO_3–NH_3–non-volatile cation (NVC) thermodynamic system, where Na^+ is used as a proxy for NVCs.

The heterogeneous uptake of N_2O_5 on aerosol surfaces leading to the production of $ClNO_2$ and HNO_3 has also been included in GEOS-Chem with the parameterizations for $\gamma_{N_2O_5}$ and φ_{ClNO_2} proposed by McDuffie et al. (2018b, a) by default (hereinafter referred to as McDuffie parameterization). McDuffie parameterization is the first field-based empirical parameterization derived from the framework proposed in multiple laboratory studies including BT09 (Anttila et al., 2006; Bertram and Thornton, 2009; Riemer et al., 2009) to account for the uptake dependence on aerosol water and nitrate concentrations as well as the resistance from an organic coating. The coefficients for McDuffie parameterization were derived from applying a box model to observations of N_2O_5, $ClNO_2$, O_3, and NO_x mixing ratios during the winter in the eastern US. The parameterization for $\gamma_{N_2O_5}$ accounts for both the inorganic and organic aerosol components and can be described by Eqs. (1)–(3):

$$\frac{1}{\gamma_{N_2O_5}} = \frac{1}{\gamma_{core}} + \frac{1}{\gamma_{coat}}, \tag{1}$$

$$\gamma_{core} = \frac{4V}{c \cdot S_a} K_H \times 2.14 \times 10^5 \times [H_2O] \left(1 - \frac{1}{k_a \frac{[H_2O]}{[NO_3^-]} + 1}\right), \tag{2}$$

$$\gamma_{coat} = \frac{4RT\varepsilon H_{aq} D_{aq} R_c}{cl R_p}, \tag{3}$$

where γ_{core} represents the reactive uptake of the inorganic aerosol core and γ_{coat} represents the retardation of the organic coating; c is the average gas-phase thermal velocity of N_2O_5 ($m\,s^{-1}$), V is the total particle volume concentration ($m^3\,m^{-3}$), S_a is the total particle surface area concentration ($m^2\,m^{-3}$), K_H is the unitless Henry law coefficient for N_2O_5 with a constant value of 51, $[H_2O]$ and $[NO_3^-]$ are the concentrations of aerosol liquid water content and aerosol nitrate ($mol\,L^{-1}$), respectively, and k_a is the rate constant ratio representing the competition between aerosol-phase H_2O and NO_3^- for the $H_2ONO_2^+(aq)$ intermediate and is fixed at

0.04 in Eq. (2). R is the ideal gas constant; T is the temperature (K); H_{aq} and D_{aq} are the aqueous Henry law constant and aqueous-phase diffusion coefficient of N_2O_5, respectively; ε is a linear combination of relative humidity (RH) and O : C ratio ($= 0.15 \times$ O : C $+ 0.0016 \times$ RH); and R_p, R_c, and l are the total particle radius, inorganic core radius, and organic coating thickness, respectively (m).

φ_{ClNO_2} is calculated following BT09 but is reduced by 75 % based on the observations conducted in the eastern US and offshore in spring 2015 (i.e., the WINTER aircraft campaign) (McDuffie et al., 2018b). It could be described by Eq. (4):

$$\varphi_{ClNO_2} = 0.25 \times \left(k_c \frac{[H_2O]}{[Cl^-]} + 1 \right)^{-1}, \tag{4}$$

where k_c is the rate constant ratio representing the competition between aerosol-phase H_2O and Cl^- for the $H_2ONO_2^+(aq)$ intermediate and is fixed at 1/450 here, and $[Cl^-]$ is the concentration of aerosol chloride ($mol\,L^{-1}$). For a more detailed description of the McDuffie parameterization, readers are referred to McDuffie et al. (2018b, a). Keep it in mind that the coefficients for the parameterizations in Eqs. (1)–(4) were derived to better reproduce wintertime observations in the eastern US. However, there are large uncertainties in both the values of the coefficients and functional form of the parameterizations, specifically related to their applicability to other regions.

Recently, Yu et al. (2020) proposed new parameterizations of $\gamma_{N_2O_5}$ and φ_{ClNO_2} based on BT09 to account for the dependence on aerosol water, nitrate, and chloride concentrations but with coefficients derived from uptake coefficients directly measured on ambient aerosol in two rural sites in China. The parameterizations of $\gamma_{N_2O_5}$ and φ_{ClNO_2} (hereinafter referred to as the Yu parameterization) are described by Eqs. (5) and (6), respectively.

$$\gamma_{N_2O_5} = \frac{4V}{c \cdot S_a} K_H \times 3.0 \times 10^4 \times [H_2O]$$

$$\times \left(1 - \frac{1}{k_a \frac{[H_2O]}{[NO_3^-]} + k_b \frac{[Cl^-]}{[NO_3^-]} + 1} \right) \tag{5}$$

$$\varphi_{ClNO_2} = \left(1 + k_c \frac{[H_2O]}{[Cl^-]} \right)^{-1} \tag{6}$$

Here k_b is the rate constant ratio representing the competition between aerosol-phase Cl^- and NO_3^- for the $H_2ONO_2^+(aq)$ intermediate and is fixed at 3.4. In contrast to the McDuffie parameterization, k_a and k_c in the Yu parameterization are fixed at 0.033 and 1/150, respectively.

Although both parameterizations are developed based on BT09, there are significant differences of $\gamma_{N_2O_5}$ and φ_{ClNO_2} between the McDuffie and Yu parameterizations. For $\gamma_{N_2O_5}$, the McDuffie parameterization generally follows BT09 for the calculation of the uptake on inorganic aerosols (i.e., γ_{core})

but excludes the dependence on aerosol chloride so as to better reproduce observed wintertime reactive nitrogen in the eastern US. Moreover, the parameterization accounts for the suppressive effects of the organics (i.e., γ_{coat}), which are not directly included in BT09 (Anttila et al., 2006; Riemer et al., 2009; Morgan et al., 2015). In contrast to the McDuffie parameterization, the Yu parameterization excludes the organic suppression but includes the chloride enhancement so as to better reproduce $\gamma_{N_2O_5}$ observed in China (Yu et al., 2020). It is worth mentioning that the coefficients applied in the parameterization of $\gamma_{N_2O_5}$ also differ between the McDuffie and Yu parameterizations as both are fixed to reproduce the ambient observation representing different pollution conditions. For example, k_a is equal to 0.04 in Eq. (2) but 0.033 in Eq. (5). The $\gamma_{N_2O_5}$ in the McDuffie parameterization is thus expected to be lower compared with the Yu parameterization due to the resistance from organic coating and the lack of the chloride enhancement. For φ_{ClNO_2}, both the McDuffie and Yu parameterizations are based on BT09, but with different coefficients (i.e., $k_c = 1/450$ in Eq. 4 and 1/150 in Eq. 6). Although k_c in Eq. (4) is relatively smaller, the scaling factor of 0.25 applied in Eq. (4) ultimately results in a much smaller φ_{ClNO_2} in the McDuffie parameterization compared with the Yu parameterization under the same condition. Again, keep it in mind that the McDuffie parameterization is derived from fits to observations over the eastern US (McDuffie et al., 2018a) while the Yu parameterization is fitted to observations at rural locations in China (Yu et al., 2020).

In this study, we updated the parameterizations for $\gamma_{N_2O_5}$ and φ_{ClNO_2} in the heterogeneous $N_2O_5 + Cl$ chemistry (hereinafter referred to as parameterizations for heterogeneous $N_2O_5 + Cl$ chemistry) in the GEOS-Chem with the Yu parameterization. Additional simulation cases were also performed to evaluate the representativeness of both the Yu and McDuffie parameterizations regarding the simulation of N_2O_5, $ClNO_2$, O_3, $PM_{2.5}$, and its chemical compositions in China. Detailed description of the model setup for related cases is provided below in Sect. 2.1.3.

2.1.2   Emissions

The study uses the Hemispheric Transport of Air Pollution (HTAPv2, http://www.htap.org/, last access: 14 March 2022) based on the emission of 2010 as a global anthropogenic inventory. This inventory is overwritten by a regional emission inventory MIX (with a horizontal resolution of $0.25° \times 0.25°$) over East Asia based on the emission in 2017, which is developed for the Model Inter-Comparison Study for Asia (MICS-Asia) and covers all major anthropogenic sources in 30 Asian countries and regions (Li et al., 2017). In addition, anthropogenic emissions of black carbon (BC) and organic carbon (OC) in Guangdong Province, China (20–26° N, 109–117° E), are overwritten by a more recent high-resolution inventory (9 km × 9 km) described by Huang et al. (2021). Biomass burning emissions are from the Global Fire

Table 1. Chlorine emissions in China in the model.

Sources	By default (Gg Cl a^{-1})	Updated in this study (Gg Cl a^{-1})
Sea salt Cl$^-$	6.5×10^4	6.5×10^4
Anthropogenic HCl	0	218
Biomass burning HCl	0	30
Anthropogenic Cl$_2$	0	8.9
Anthropogenic Cl$^-$	0	379
Biomass burning Cl$^-$	0	120
CH$_3$Cl*	3.8	3.8
CH$_2$Cl$_2$*	2.4	2.4
CHCl$_3$*	0.70	0.70

* Sources are shown in terms of the chemical release (e.g., +Cl, +OH, +$h\nu$).

Emissions Database (GFED4) (Van et al., 2010) with a 3 h time resolution. The biogenic emissions of VOCs are calculated based on the Model of Emissions of Gases and Aerosols from Nature (MEGAN2.1) (Guenther et al., 2006).

Table 1 lists Cl emissions from all sources in the model. The global tropospheric chlorine by default in the model is mainly from the mobilization of Cl$^-$ from SSA distributed over two size bins (fine and coarse modes) (Wang et al., 2019), which is computed online as the integrals of the size-dependent source function depending on wind speeds and sea surface temperatures (Jaeglé et al., 2011). During the simulation year of 2018, SSA contributes 6.5×10^4 Gg Cl$^-$, most of which however is distributed over the ocean due to its relatively short lifetime (~ 1.5 d) (Choi et al., 2020). The release of atomic Cl from organic chlorine (CH$_3$Cl, CH$_2$Cl$_2$, and CHCl$_3$) via oxidation by OH and Cl is also included in the model by default. These organic chlorine gases are mainly of biogenic marine origin (Simmonds et al., 2006), with a mean tropospheric lifetime longer than 250 d (X. Wang et al., 2020), and are simulated in the model by imposing fixed surface concentrations as described by Schmidt et al. (2016). Total emissions of Cl atoms from CH$_3$Cl, CH$_2$Cl$_2$, and CHCl$_3$ are calculated to be 3.8, 2.4, and 0.70 Gg Cl a^{-1}, respectively.

Considering the importance of anthropogenic chlorine in China, we have further updated chlorine inventories in the model to account for anthropogenic HCl, Cl$_2$ and fine particulate Cl$^-$, and biomass burning HCl and Cl$^-$ emissions (also shown in Tables 1 and S1 in the Supplement). For fine particulate Cl$^-$ from both anthropogenic and biomass burning, the emissions are estimated based on PM$_{2.5}$ emissions from MIX and GFED4 inventories combined with the emission ratios of fine particulate Cl$^-$ versus PM$_{2.5}$ for different emission sectors adopted from the study of Fu et al. (2018). Estimated Cl$^-$ emissions from anthropogenic and biomass burning are 379 and 120 Gg, respectively, comparable to the results of 486 Gg in total for the year of 2014 by Fu et al. (2018). The anthropogenic emissions of HCl and Cl$_2$ are from ACEIC (Anthropogenic Chlorine Emissions Inventory

for China) (Liu et al., 2018) and are estimated to be 218 and 8.9 Gg Cl in China, respectively. For HCl from biomass burning, the emission factors from Lobert et al. (1999) are used for different types of biomass provided in GFED4, and a total emission of 30 Gg Cl is obtained in China in 2018. Total implemented chlorine emission for the simulation year of 2018 is 756 Gg Cl.

Figure 1 shows the distribution of Cl emissions from the sources mentioned above. Anthropogenic and biomass burning emissions of HCl are concentrated in the Northeast Plain, North China Plain, Yangtze River Delta, and Sichuan Basin and are up to 320 kg Cl km^{-2} a^{-1} in the Sichuan Basin. Emissions of HCl are low in south China, mainly due to the low chlorine content of coal in these regions (Hong et al., 2020). The relative contribution of biomass burning to total HCl emissions in China is 14 % on average but could become dominant in the Northeast Plain due to the discrepancies in the spatial distributions of anthropogenic and biomass burning emissions. The anthropogenic Cl$_2$ emissions have a similar spatial distribution to that of HCl but are 1 order of magnitude lower than HCl emissions. The distribution of non-sea-salt Cl$^-$ emissions is also similar to that of HCl and Cl$_2$, except that non-sea-salt Cl$^-$ emissions are also high in central China. In contrast, emissions of sea salt Cl$^-$ (Fig. S1 in the Supplement) are mainly distributed over the ocean, implying limited influences inland due to rapid deposition during transport. The spatial distributions of different organic chlorine sources are similar, with maximums (~ 0.5 kg Cl km^{-2} a^{-1}) in coastal regions (Fig. S1).

2.1.3 Model setup for different simulation cases

In this study, we conducted a series of simulation cases to investigate the effects of chlorine chemistry on air quality in China, the role of N$_2$O$_5$–ClNO$_2$ chemistry, and the associated sensitivities to chlorine emissions as well as the parameterizations for N$_2$O$_5$–ClNO$_2$ chemistry. A detailed model setup for those cases is listed in Table 2. The Base case is the one with all updates in this study, including additional chlorine sources from anthropogenic and biomass burning emissions as well as N$_2$O$_5$ uptake and ClNO$_2$ production represented by the Yu parameterization. The NoEm case is conducted with a similar setup as the Base case but only includes chlorine emissions from SSA and organic chlorine sources so as to evaluate the model improvement originating from the updated chlorine emissions through the comparison with the Base case. The McDuffie case is also performed using the McDuffie instead of Yu parameterization for $\gamma_{N_2O_5}$ and φ_{ClNO_2} while keeping others the same as the Base case so as to evaluate the discrepancies originating from different parameterizations for the heterogeneous N$_2$O$_5$ + Cl chemistry.

In addition, while keeping others the same as the Base case, the NoHet case sets φ_{ClNO_2} to zero (Eq. 6) and removes the enhancement of N$_2$O$_5$ uptake from aerosol chloride (i.e., [Cl$^-$] = 0 in Eq. 5). The comparison between the
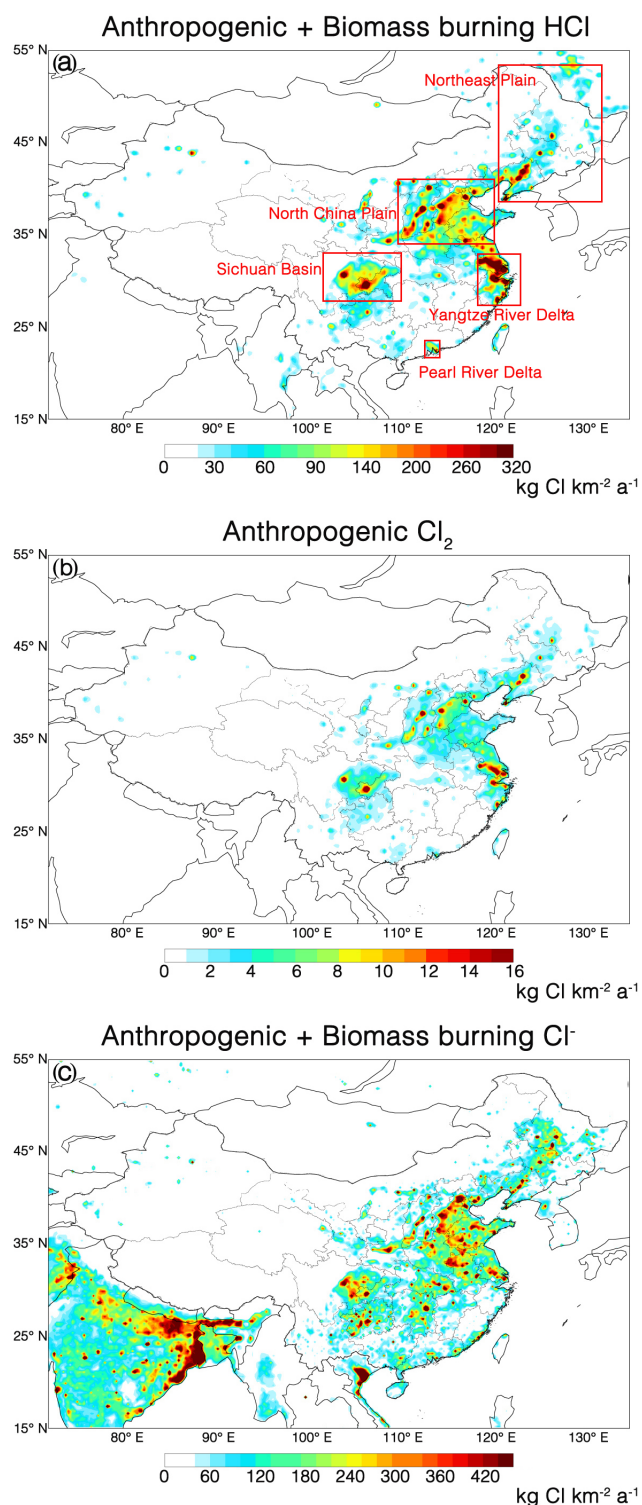
Figure 1. Annual emissions of **(a)** HCl, **(b)** Cl_2, and **(c)** non-sea-salt Cl^-. Locations of the Northeast Plain, North China Plain, Yangtze River Delta, Pearl River Delta, and Sichuan Basin are highlighted by red boxes in **(a)**.

Base and NoHet cases could thus evaluate the importance of the heterogeneous $N_2O_5 + Cl$ chemistry (i.e., the model sensitivities to a smaller gamma N_2O_5 and zero $ClNO_2$ production). Similarly, combined with three more sensitivity cases (NoChem, NoEmHet, and NoAll; see details in Table 2), the study provides an overall evaluation of the importance of tropospheric chlorine chemistry as well as its sensitivities to chlorine emissions and the parameterizations for the heterogeneous $N_2O_5 + Cl$ chemistry in the model.

2.2 Observations

Multiple observed datasets were applied in this study to evaluate the performance of GEOS-Chem simulation, including the concentrations of chemical compositions of $PM_{2.5}$ from three representative sites, located in south (Guangzhou, 23.14° N, 113.36° E), east (Dongying, 37.82° N, 119.05° E), and north (Gucheng, 37.36° N, 115.96° E) China, respectively (Fig. S2). Concentrations of SO_4^{2-}, NO_3^-, NH_4^+, Cl^-, and organic matter (OM) in $PM_{2.5}$ were measured by a high-resolution time-of-flight aerosol mass spectrometer (HR-ToF-AMS; Aerodyne Research Inc., USA; Decarlo et al., 2006) from 2 October to 18 November 2018 (with a time resolution of 1 min) at the Guangzhou site (W. Chen et al., 2021), and from 18 March to 21 April 2018 (with a 1 min time resolution) at the Dongying site. Concentrations of these species were measured by an Aerodyne quadruple aerosol chemical speciation monitor (ACSM; Aerodyne Research Inc., USA; Ng et al., 2011) from 11 November to 18 December 2018, with a time resolution of 2 min at the Gucheng site (Li et al., 2021).

Concentrations of N_2O_5 and $ClNO_2$ (with a time resolution of 1 min) were also measured at the Guangzhou site by a chemical ionization mass spectrometer (CIMS, THS Instruments Inc., Atlanta; Kercher et al., 2009) from 25 September to 12 November 2018 (Ye et al., 2021). To have a thorough evaluation of the representativeness of different parameterizations for $\gamma_{N_2O_5}$ and φ_{ClNO_2}, observations of $ClNO_2$ and N_2O_5 at six more sites across China from previous studies (see Table S2 and Fig. S2) are also used in this study. It should be noted that model results sampled at those sites for comparison were simulated in the same months but different years while ignoring the uncertainties associated with the interannual variability.

In addition, we also use observed hourly data of O_3 and $PM_{2.5}$ published by the China National Environmental Monitoring Center (CNEMC, http://www.cnemc.cn/sssj/, last access on 20 June 2021) to evaluate the model's overall performance in China. The network was launched in 2013 as part of the Clean Air Action Plan and included ~1500 stations located in 370 cities by 2018 (Fig. S2).

Table 2. Model setup of all simulation cases.

Cases	N$_2$O$_5$ uptake ($\gamma_{N_2O_5}$)	ClNO$_2$ production (φ_{ClNO_2})	Other tropospheric chlorine chemistry	Anthropogenic and biomass burning inorganic chlorine emissions
Base	Yu et al. (2020)	Yu et al. (2020)	Full	Yes
McDuffie	McDuffie et al. (2018a, b)	McDuffie et al. (2018a, b)	Full	Yes
NoEm	Yu et al. (2020)	Yu et al. (2020)	Full	None
NoHet	Yu et al. (2020) but with [Cl$^-$] $= 0$	None	Full	Yes
NoChem	Yu et al. (2020) but with [Cl$^-$] $= 0$	None	None	Yes
NoEmHet	Yu et al. (2020) but with [Cl$^-$] $= 0$	None	Full	None
NoAll	Yu et al. (2020) but with [Cl$^-$] $= 0$	None	None	None

3 Results and discussion

3.1 Improved model performance with updated chlorine emissions and parameterizations for the heterogeneous N$_2$O$_5$ + Cl chemistry

Figure 2 shows time series of observed and simulated Cl$^-$ concentrations at the Guangzhou, Dongying, and Gucheng sites. The observations show the lowest Cl$^-$ concentrations at the Guangzhou site ($0.55 \pm 0.52\,\mu g\,m^{-3}$), although the site is the closest to the ocean among all three sites, while the highest concentrations ($4.7 \pm 3.3\,\mu g\,m^{-3}$) are observed at the Gucheng site, away from the sea. Moderate concentrations of Cl$^-$ are observed at the Dongying site, around $1.1 \pm 0.82\,\mu g\,m^{-3}$. The relatively higher concentrations observed inland again suggest the dominance of non-sea-salt Cl$^-$ in China, as mentioned before in the Introduction.

The comparison between observations and simulated results from the NoEm case shows a serious underestimate of Cl$^-$ concentrations, with normalized mean bias (NMB) ranging from -96% to -79%, suggesting the missing of significant chlorine sources in addition to sea salt chlorine. In contrast, the Base case with updated chlorine emissions exhibits much higher Cl$^-$ concentrations and can successfully reproduce observations, with average concentrations of 0.77 ± 0.54, 0.71 ± 0.52, and $4.5 \pm 2.4\,\mu g\,m^{-3}$ (NMB $= 39\%$, -36%, and -4.7%) at the Guangzhou, Dongying, and Gucheng sites, respectively. The increase in Cl$^-$ concentrations in the Base case compared with the NoEm case is the most significant at the Gucheng site, by a factor of 24 (from 0.19 to $4.5\,\mu g\,m^{-3}$ on average). The slight underestimates at the Dongying site in the Base case could be to some extent explained by the bias in GFED4, which underestimates emissions from agricultural fires due to their small size and short duration as suggested by the study of Zhang et al. (2020). In spite of that, the model with the Base case reproduces the overall distribution of the observed particulate chloride concentrations in China well. The correlation coefficients (r) between observed and model results at the three sites also increase from -0.05–0.61 in the NoEm case

to 0.40–0.71 in the Base case. The significant improvement in the model performance again suggests sources other than SSA play a key role in Cl$^-$ concentrations in China.

The comparison between observed and simulated N$_2$O$_5$ (Fig. 3a) shows that NMB for the NoEm case is -58%, 150%, 108%, and 25% at the Guangzhou, Wangdu, Taizhou, and Mount Tai sites, respectively. In contrast, the corresponding NMB for the Base case is much smaller, -57%, 48%, 91%, and 18%, respectively. The improvement in the Base case is apparent at most sites, implying that additional chlorine emissions could effectively increase the uptake coefficient of N$_2$O$_5$ in the Yu parameterization. As shown in Fig. S3, although the values of $\gamma_{N_2O_5}$ between the Base and NoEm cases are similar over the ocean, the Base case has relatively higher $\gamma_{N_2O_5}$ over China compared with the NoEm case (0.016 vs. 0.014 on an annual mean basis). Little improvement is found at the Guangzhou site (-58% in the NoEm case vs. -57% in the Base case). Previous studies also found an underestimation of N$_2$O$_5$ in the Pearl River Delta, which could be partly explained by the underestimation of the sources (e.g NO$_2$) and/or the overestimation of the sink of N$_2$O$_5$ there (Dai et al., 2020; Li et al., 2016).

The N$_2$O$_5$ results from the McDuffie case, which uses the McDuffie parameterization (a default setting in GEOS-Chem; see Sects. 2.1.1 and 2.1.3) instead of the Yu parameterization are also shown in Fig. 3a. The NMB for the McDuffie case is -53%, 154%, 143%, and 37% at the Guangzhou, Wangdu, Taizhou, and Mount Tai sites, respectively. The comparison between the McDuffie and Base cases indicates that the Yu parameterization can reproduce observed N$_2$O$_5$ better in China in general, while the McDuffie parameterization tends to overestimate N$_2$O$_5$ concentrations. The overestimate of N$_2$O$_5$ in the McDuffie parameterization suggests the potential underestimate in the corresponding $\gamma_{N_2O_5}$. As shown Fig. S3, the value of $\gamma_{N_2O_5}$ from the McDuffie case is much smaller than that from the Base case (0.0071 vs. 0.016 averaged over China).

The underestimate in $\gamma_{N_2O_5}$ from the McDuffie case could to a large extent be explained by the suppressive effect of organic coatings (γ_{coat}) as discussed above in Sect. 2.1.1.
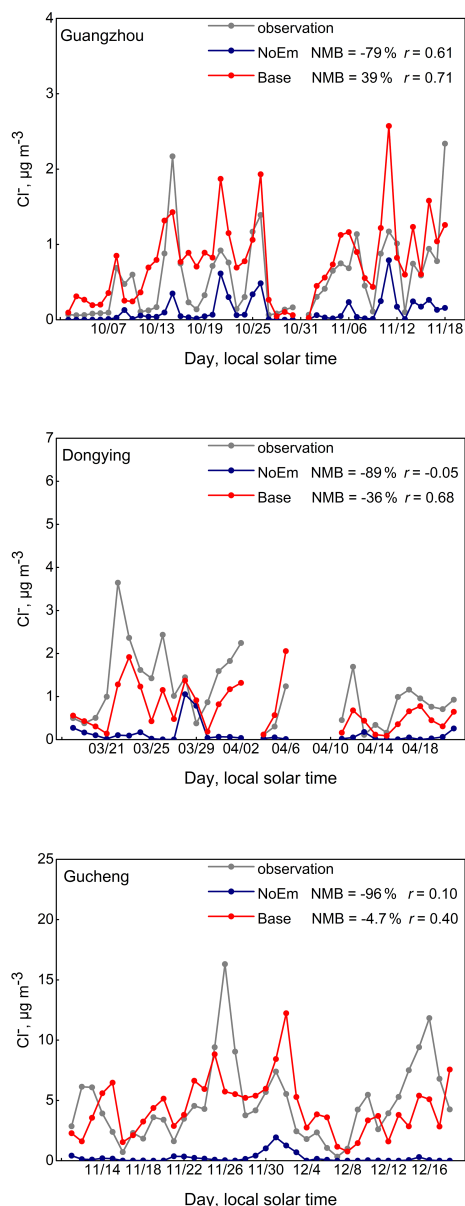
Figure 2. Time series of simulated and observed particulate Cl^- concentrations at the Guangzhou, Dongying, and Gucheng sites.

The magnitude of the organic suppression is highly dependent on many factors (e.g., organic composition, particle phase state) and thus remains poorly quantified (Griffiths et al., 2009; Gross et al., 2009; Thornton et al., 2003). Although many studies have shown that organic aerosol can suppress the N_2O_5 uptake (Anttila et al., 2006; Riemer et al., 2009), the level of organic suppression may be overpredicted in the currently implemented parameterization attributed to the poorly quantified and/or unknown factors (e.g., Morgan et al., 2015). For example, some studies found that ignoring the difference between water-soluble and water-insoluble organics may lead to an upper limit for the suppressive ef-

fect of organic coatings and consequently an underestimate in the solubility and diffusivity of N_2O_5 in organic matter (Chang et al., 2016; Yu et al., 2020). Although γ_{coat} in the McDuffie parameterization is calculated as a function of organic aerosol O : C ratio and RH (see Eq. 2), which could increase with higher RH and higher O : C ratio, it may still overpredict the suppressive role of organic coatings in China. On the other hand, the study by Yu et al. (2020) found that excluding the organic coating best reproduced uptake coefficients observed in China. In addition, the underestimate in $\gamma_{N_2O_5}$ in the McDuffie parameterization in China could also be to some extent explained by the lack of the chloride enhancement (also discussed in Sect. 2.1.1). It is worth noting that the evaluation here is specific to China, and the differences between the Yu and McDuffie parameterizations have not been evaluated elsewhere.

For the comparison of $ClNO_2$ (Fig. 3b), we use the mean nighttime (excluding the data at a local time of 10:00–16:00) maximum mixing ratio, as suggested by Wang et al. (2019). Observed $ClNO_2$ is high in Guangzhou (1121 pptv) and Wangdu ($\sim$ 990 pptv), followed by Changping ($\sim$ 500 pptv) and Beijing ($\sim$ 430 pptv). The lowest concentrations are obtained at Mount Tai and Tai Mo Shan ($\sim$ 150 and 120 pptv, respectively) due to relatively clean conditions at high altitude. The comparison between observed and simulated $ClNO_2$ at different sites also suggests a better model performance for the Base case, with NMB in the range of -28%– 22 %, compared with the NMB of -77% to -31% and -59% to -36% for the NoEm and McDuffie cases, respectively. The difference in $ClNO_2$ concentrations is mainly associated with distinct φ_{ClNO_2} values among different cases. As shown in Fig. S4, the value of φ_{ClNO_2} is significantly higher in the Base case (0.36 averaged over China) than in the NoEm (0.14) and McDuffie (0.11) cases. The large difference between the NoEm and Base cases again emphasizes the important role of non-sea-salt chlorine in the formation of $ClNO_2$. The overall underestimates in the McDuffie parameterization on the other hand may suggest that the scaling factor of 0.25 applied to φ_{ClNO_2} in Eq. (4) is too much for the atmospheric condition in China. More field measurements and model evaluations are required to come up with a more precise parameterization better representing φ_{ClNO_2} in China.

Overall, with updated chlorine emissions and Yu parameterization for $\gamma_{N_2O_5}$ and φ_{ClNO_2}, the Base case agrees better with both the magnitude and the spatial variation in observed N_2O_5 and $ClNO_2$ in China. The differences in $\gamma_{N_2O_5}$ and φ_{ClNO_2} could also affect the ratios of $ClNO_2$ to HNO_3. As shown in Fig. S5, the value of $ClNO_2/HNO_3$ is the highest from the Base case (9.8 % averaged in China and up to 47 % in the Sichuan Basin on an annual mean basis), followed by the McDuffie (4.7 % averaged in China and up to 18 % in the Sichuan Basin) and NoEm (3.1 % averaged in China and up to 12 % in coastal regions) cases.
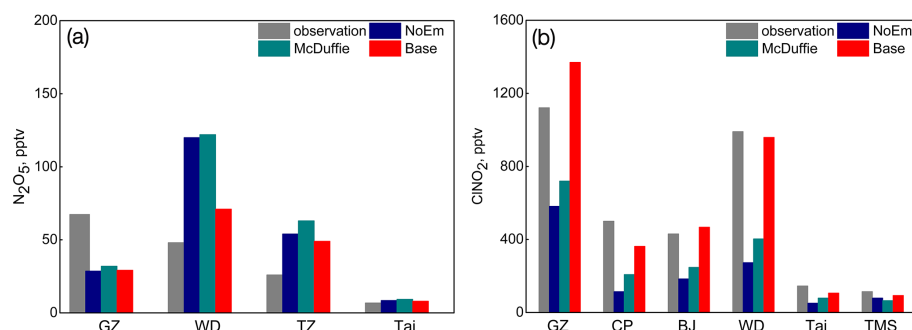
Figure 3. Comparison of observed and simulated **(a)** averaged N$_2$O$_5$ concentrations and **(b)** mean nighttime maximum mixing ratio of ClNO$_2$ concentrations at different sites. The simulation definitions are provided in Table 2. GZ: Guangzhou; WD: Wangdu; TZ: Taizhou; Tai: Mount Tai; CP: Changping; BJ: Beijing; TMS: Tai Mo Shan.
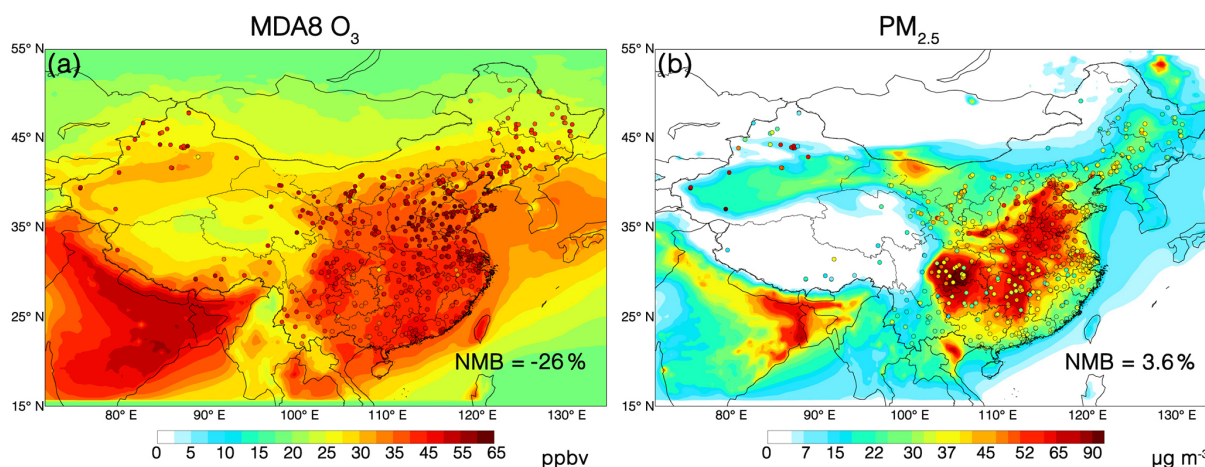
Figure 4. Annual mean surface concentrations of **(a)** MDA8 O$_3$ and **(b)** PM$_{2.5}$ over China in 2018. GEOS-Chem model values from the Base case are shown as contours. Observations from the China National Environmental Monitoring Center (CNEMC) are shown as circles.

To further elucidate how the model behaves in reproducing the spatial distribution of ozone and PM$_{2.5}$ through the incorporation of the additional chlorine emissions and Yu parameterization for the heterogeneous N$_2$O$_5$ + Cl chemistry, simulated MDA8 O$_3$ and PM$_{2.5}$ from different cases were compared with observations across China. Figure 4 shows simulated annual mean MDA8 O$_3$ and PM$_{2.5}$ in 2018 in China from the Base case compared with the observations from CNEMC (China National Environmental Monitoring Center, introduced in Sect. 2.2). The observed annual mean MDA8 O$_3$ and PM$_{2.5}$ are 49 ppbv and 39 µg m^{-3}, respectively, in 2018 in China. Model results from the Base case could generally reproduce observed spatial and seasonal variations in annual mean MDA8 O$_3$ and PM$_{2.5}$ concentrations, with NMB of −26 % and 3.6 % and r of 0.83 and 0.81, respectively (Fig. S6).

Table 3 also summarized the model performance on both annual and seasonal scales regarding the simulation of O$_3$ and PM$_{2.5}$ from different cases. For the comparison with observed MDA8 O$_3$, although different simulation cases show a similar range of r, the Base case tends to have a slightly smaller bias in general, with NMB of −26 % on an annual average (−49 % to −5.5 % on seasonal mean) vs. −28 % (−54 % to −5.9 %) in the NoEm case and −27 % (−53 % to −5.2 %) in the McDuffie case. For the comparison with observed PM$_{2.5}$, the NMB bias from the Base case is 3.6 % on an annual average (−6.3 %–28 % seasonal mean). Compared with the NoEm case, there is some improvement in summer (5.0 % vs. 3.9 %) and winter (−7.9 % vs. −4.3 %) but slightly larger bias in autumn (26 % vs. 28 %). The McDuffie case on the other hand produces slightly higher PM$_{2.5}$ concentrations, with NMB of 5.6 %. Regarding the chemical compositions of PM$_{2.5}$ (Table S3), although the model performance varies with sites and species, the Base case demonstrates better agreement with observations compared with the NoEm and McDuffie cases in general.

On the whole, the model performance is better with the additional anthropogenic and biomass burning chlorine emissions combined with the Yu parameterization for the heterogeneous N$_2$O$_5$ + Cl chemistry. Therefore, the follow-

Table 3. Normalized mean bias (NMB) and correlation coefficients (r) between observed and simulated MDA8 O_3 and $PM_{2.5}$ concentrations during 2018 in China.

Species	Time	Base		McDuffie		NoEm	
		NMB	r	NMB	r	NMB	r
MDA8 O_3	Annual	-26%	0.83	-27%	0.83	-28%	0.82
	MAM[a]	-35%	0.87	-36%	0.87	-36%	0.87
	JJA[b]	-5.5%	0.50	-5.2%	0.48	-5.9%	0.48
	SON[c]	-24%	0.79	-26%	0.78	-28%	0.76
	DJF[d]	-49%	0.81	-53%	0.80	-54%	0.80
$PM_{2.5}$	Annual	3.6%	0.81	5.6%	0.81	2.3%	0.80
	MAM	-6.3%	0.52	-4.9%	0.53	-6.2%	0.52
	JJA	3.9%	0.70	4.6%	0.70	5.0%	0.70
	SON	28%	0.79	32%	0.80	26%	0.79
	DJF	-4.3%	0.82	-2.6%	0.82	-7.9%	0.82

[a] March, April, and May (spring). [b] June, July, and August (summer). [c] September, October, and November (autumn). [d] December, January, and February (winter).

ing investigation of the impacts of chlorine chemistry on air quality in China as well as their sensitivities to chlorine emissions and parameterizations for the heterogeneous $N_2O_5 + Cl$ chemistry is mainly based on the Base case.

## 3.2 Impacts of tropospheric chlorine chemistry on air quality and the role of the heterogeneous $N_2O_5 + Cl$ chemistry

To comprehensively quantify the importance of chlorine chemistry, we conducted a sensitivity case in which all related tropospheric chlorine chemistry was turned off (NoChem, also listed in Table 2). The differences between the Base and NoChem cases (Figs. 5 and S7) could thus represent the impact of the chlorine chemistry. The comparison shows that chlorine chemistry could increase annual mean nighttime max $ClNO_2$ surface concentrations by 243 pptv averaged in China (up to 1548 pptv in the Sichuan Basin). The increase in annual mean Cl atoms is 1.7×10^3 molec. cm^{-3} averaged in China (up to 7×10^3 molec. cm^{-3} in coastal regions). The increased Cl atoms could react with VOCs (especially alkanes), producing more peroxy radicals, including organic peroxy radicals (RO_2) and hydroperoxyl radicals (HO_2). As shown in Fig. S7 (a), the chlorine chemistry could increase annual mean HO_2 concentrations by 1.6×10^6 molec. cm^{-3} averaged in China (up to 8.6×10^6 molec. cm^{-3} in the coastal regions). In the presence of NO, the peroxy radicals recycle OH while they oxidize NO to NO_2. The subsequent photolysis of NO_2 could further lead to more O_3 production and consequently also more OH (Osthoff et al., 2008; Riedel et al., 2014; Simpson et al., 2015). On the other hand, the recycling of NO_x back into the atmosphere associated with the photolysis of $ClNO_2$ could also lead to more O_3 production. The results here show a significant increase in sur-

face annual mean OH (Fig. S7b) and MDA8 O_3 (Fig. 5c) by 3.8×10^4 molec. cm^{-3} and 1.1 ppbv, respectively, averaged in China (up to 1.2×10^5 molec. cm^{-3} and 4.5 ppbv, respectively in the Sichuan Basin). In contrast, annual mean $PM_{2.5}$ surface concentrations are decreased by 0.91 µg m^{-3} averaged in China (up to 7.9 µg m^{-3} in the Sichuan Basin), mainly due to the decrease in NO_3^- and NH_4^+ (up to 6.4 and 1.9 µg m^{-3}, respectively), although SO_4^{2-} concentrations are increased slightly by up to 1.2 µg m^{-3} in the Sichuan Basin (Fig. S7).

Both global and regional studies suggested that the heterogeneous $N_2O_5 + Cl$ chemistry can enhance O_3 production through the production of Cl atoms and the recycling of NO_x (Li et al., 2016; Sarwar et al., 2014; Wang et al., 2019). Therefore, we further investigate the role that the heterogeneous $N_2O_5 + Cl$ chemistry plays in tropospheric chlorine chemistry through the comparison between the Base and NoHet (Figs. 6 and S8) cases. Keep it in mind that the comparison mainly assesses the impact of $ClNO_2$ production, namely the uptake of N_2O_5 on chloride aerosol, not the general role of N_2O_5 heterogeneous chemistry. The comparison illustrates that the heterogeneous $N_2O_5 + Cl$ chemistry could result in a significant production of $ClNO_2$, reaching 600–1400 pptv for annual mean nighttime max surface concentrations in the North China Plain and up to 1546 pptv in the Sichuan Basin. The change in the surface concentrations of Cl atoms (an annual mean increase of $1–4 \times 10^3$ molec. cm^{-3} in central and eastern China) is mainly due to the photolysis of $ClNO_2$ and accounts for 74 % of total change in annual mean Cl atoms due to all tropospheric chlorine chemistry in China, which is consistent with the results from the previous study by Liu et al. (2017).

In addition to the production of Cl atoms, the $ClNO_2$ formation also affects the partitioning of NO_y from HNO_3 into more reactive forms (e.g., NO_x and $ClNO_2$) through
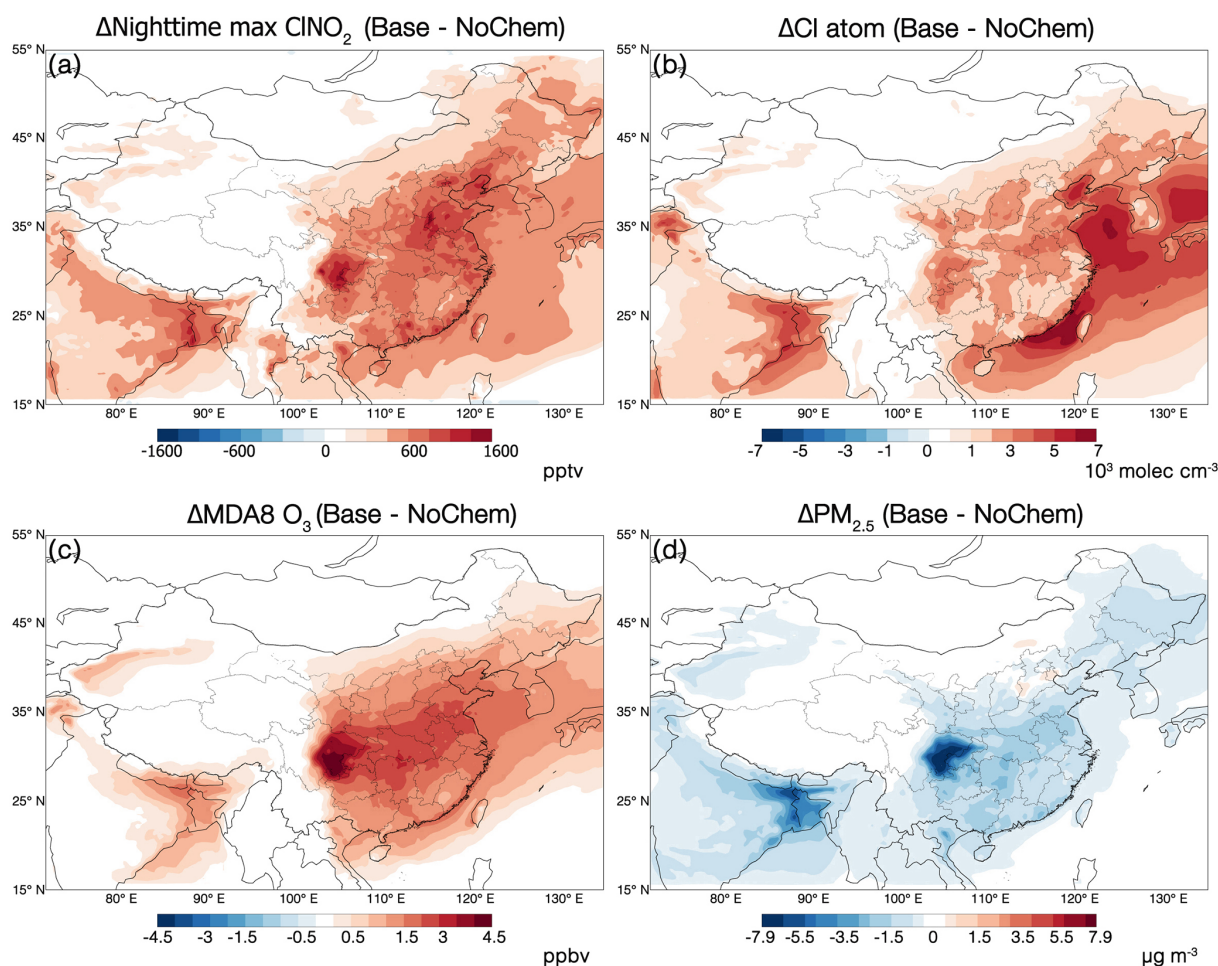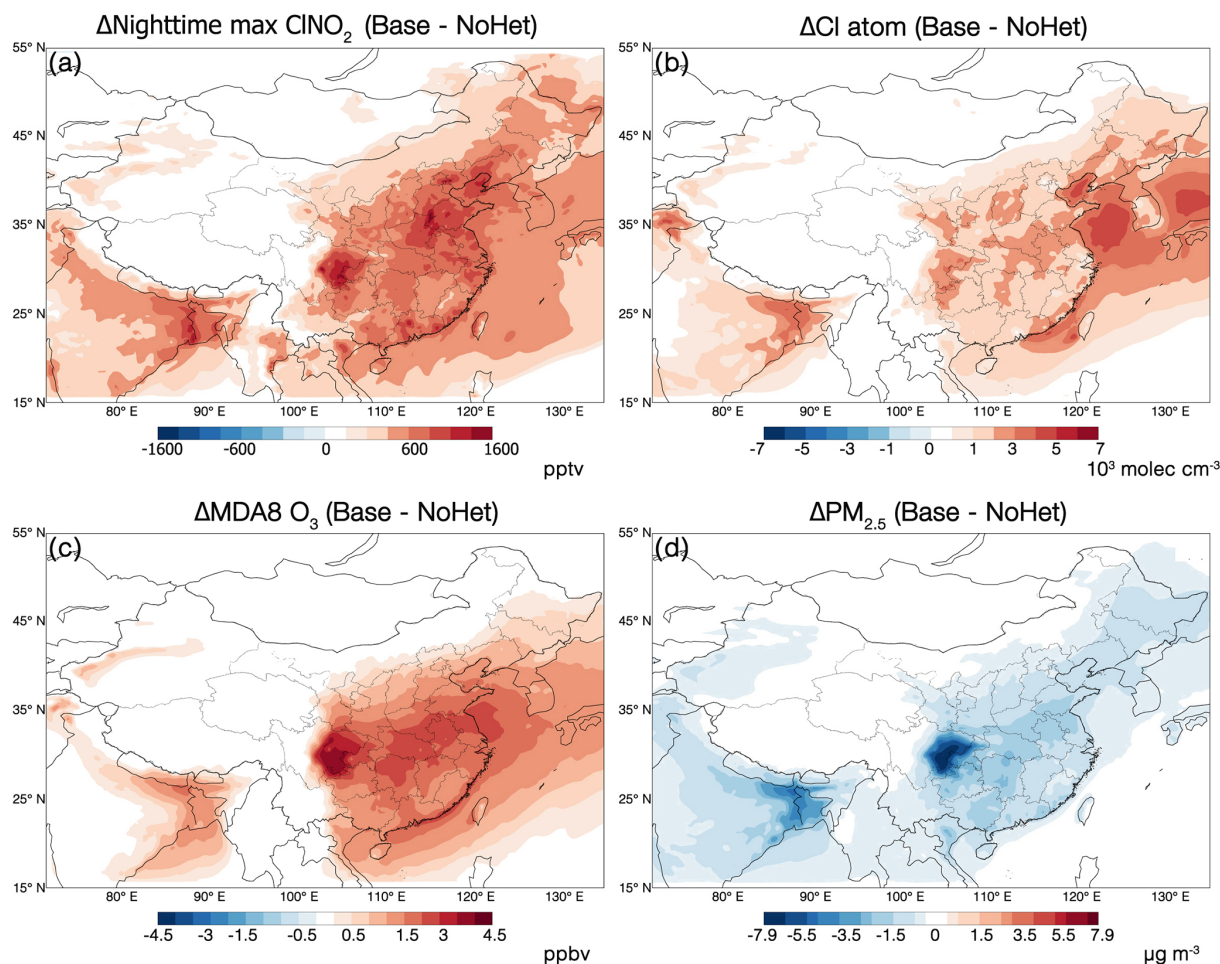
Figure 5. Effects of chlorine chemistry on annual mean surface concentrations of **(a)** nighttime max $ClNO_2$, **(b)** Cl atoms, **(c)** MDA8 O_3, and **(d)** $PM_{2.5}$ in China, estimated as the differences between the Base and NoChem cases.

the recycling of NO_x and is therefore of great importance in atmospheric chemistry (Bertram et al., 2013; Li et al., 2016; S. Wang et al., 2020). To analyze the impact of the heterogeneous $N_2O_5 + Cl$ chemistry on NO_y partitioning, Fig. S9 shows the change in the ratios of NO_x to NO_y and NO_3^- to NO_y as the difference between the Base and NoHet cases. Since $ClNO_2$ could be treated as a reservoir for reactive nitrogen at night, we include $ClNO_2$ as part of NO_x in the calculation ($NO_x = NO + NO_2 + ClNO_2$ and $NO_y + NO + NO_2 + ClNO_2 + HNO_3 + 2 \times N_2O_5 + NO_3 + HONO + HNO_4 + NO_3^- +$ various organic nitrates). The results show that due to the $ClNO_2$ production, the ratios of NO_x to NO_y increase by 1.8 % averaged in China and up to 5.4 % in the Sichuan Basin, Northeast Plain, and North China Plain on an annual mean basis. Meanwhile, the ratios of NO_3^- to NO_y decrease by 1.1 % averaged in China and up to 5.1 % in the Sichuan Basin on an annual mean basis.

Consequently, the annual mean MDA8 O_3 surface concentrations are increased by 1.5–3 ppbv in central and eastern China and up to 3.8 ppbv in the Sichuan Basin, accounting

for 83 % of total change in annual mean MDA8 O_3 due to all tropospheric chlorine chemistry in China. It is interesting to note that while MDA8 O_3 surface concentrations show maxima in summer and minima in winter in general, the influence of the heterogeneous $N_2O_5 + Cl$ chemistry on O_3 concentrations exhibits a different seasonality. The increase in seasonal mean MDA8 O_3 concentrations is the largest in winter (by up to 6.5 ppbv in the Sichuan Basin) but is less than 1.5 ppbv in summer. This is because of more accumulation of N_2O_5 and $ClNO_2$ in dark conditions in long winter nights (Sarwar et al., 2014).

There is also an obvious decrease in the annual mean surface concentrations of $PM_{2.5}$ attributed to the heterogeneous $N_2O_5 + Cl$ chemistry, ranging from 1.5 to 4.5 $\mu g\,m^{-3}$ in central and eastern China (accounting for 90 % of total change in annual mean $PM_{2.5}$ due to all tropospheric chlorine chemistry in China). The decrease is more significant in autumn and winter in China, with a range of 3.5–5.5 $\mu g\,m^{-3}$ in central and eastern China and up to 11 $\mu g\,m^{-3}$ in the Sichuan Basin. In contrast, the decrease in $PM_{2.5}$ is less than 2 $\mu g\,m^{-3}$

Figure 6. Effects of the heterogeneous N$_2$O$_5$ + Cl chemistry on annual mean surface concentrations of **(a)** nighttime max ClNO$_2$, **(b)** Cl atom, **(c)** MDA8 O$_3$, and **(d)** PM$_{2.5}$ in China, estimated as the differences between the Base and NoHet cases.

in summer in China. The change in PM$_{2.5}$ is mainly due to the decrease in NO$_3^-$ (up to 6.2 µg m^{-3} in the Sichuan Basin on an annual average). In addition, NH$_4^+$ is also decreased by up to 1.8 µg m^{-3} in the Sichuan Basin annually on average, following the pattern of ΔNO$_3^-$. This is because NH$_3$ is in excess in most regions in China (Xu et al., 2019), and the formation of ClNO$_2$ via Reaction (R2) could hinder the formation of HNO$_3$ and shift the partitioning between NH$_3$ and NH$_4^+$ towards NH$_3$. Unlike the change in NO$_3^-$ and NH$_4^+$, the heterogeneous N$_2$O$_5$ + Cl chemistry increases surface SO$_4^{2-}$ concentration slightly, which could be explained by the enhancements of atmospheric oxidation associated with the increase in Cl atoms, OH, and O$_3$, facilitating the formation of secondary aerosols (Sarwar et al., 2014).

On the other hand, the effect of tropospheric chlorine chemistry without the heterogeneous N$_2$O$_5$ + Cl chemistry is much smaller (Fig. S10, the comparison between the NoHet and NoChem cases), leading to an increase of up to 0.7 ppbv in inland China and a decrease of 0.3–0.5 ppbv in coastal regions for annual mean MDA8 O$_3$ concentrations. The increase is probably associated with Cl atoms from photolysis of gas-phase chlorine, especially non-sea-salt Cl$_2$ in inland China, while the decrease at coastal regions is mainly due to catalytic production of bromine and iodine radicals originating from sea salt aerosols. The comparison demonstrates the dominance of the heterogeneous N$_2$O$_5$ + Cl chemistry in total tropospheric chlorine chemistry in China.

3.3 The effect of heterogeneous N$_2$O$_5$ + Cl chemistry in response to chlorine emissions

Since both $\gamma_{N_2O_5}$ and φ_{ClNO_2} in the Yu parameterization are highly dependent on [Cl$^-$], the effect of the heterogeneous N$_2$O$_5$ + Cl chemistry on air quality is thus sensitive to chlorine emissions. Figure 7 shows the effects of the additional chlorine emissions from anthropogenic and biomass burning sources on annual mean surface concentrations of different species (Cl$^-$, Cl atoms, OH, MDA8 O$_3$, PM$_{2.5}$, and NO$_3^-$) in China, calculated as the differences between the Base and the NoEm cases. With the implementation of the
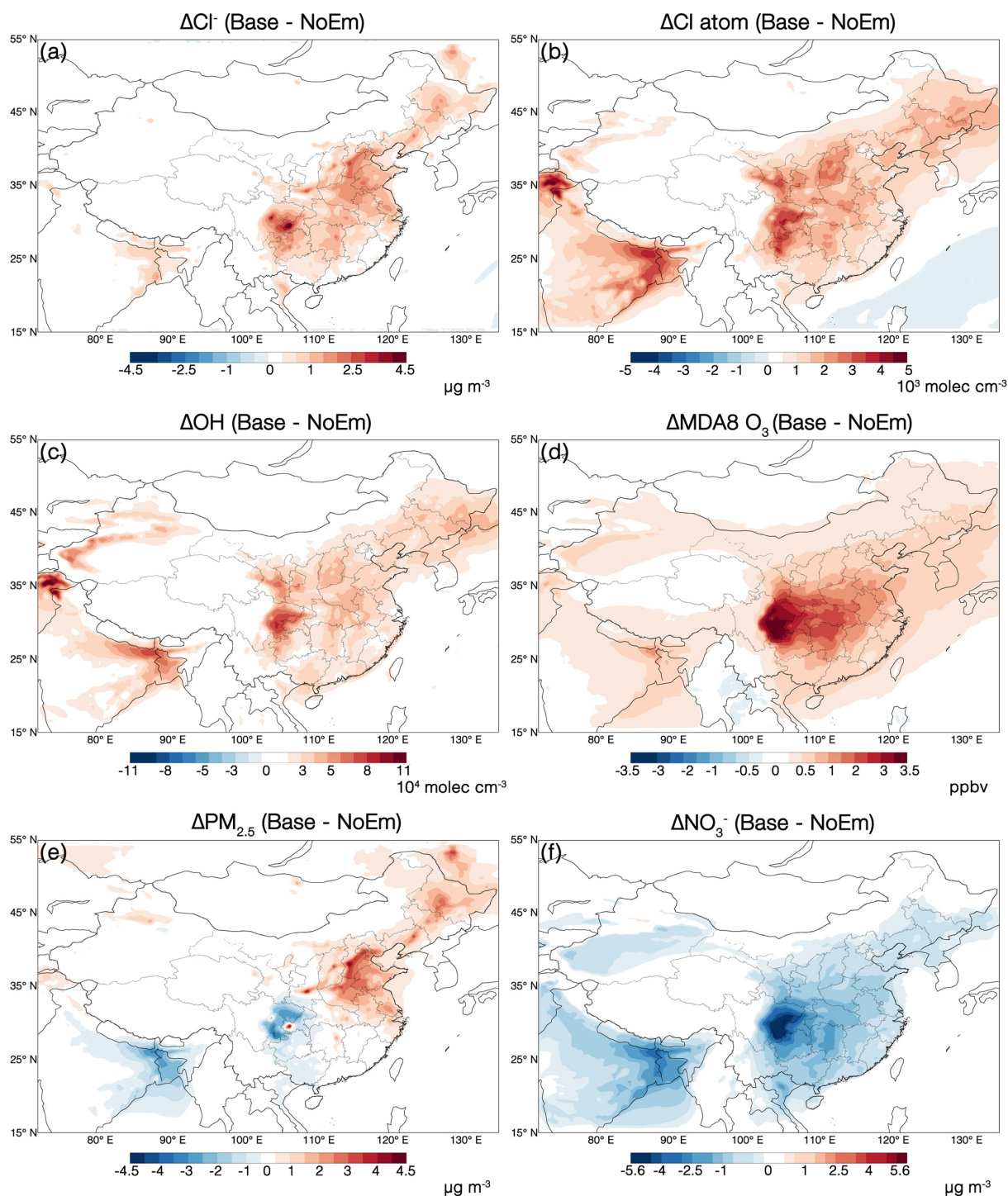
Figure 7. Effects of anthropogenic and biomass burning chlorine emissions on annual mean surface concentrations of (**a**) Cl$^-$, (**b**) Cl atoms, (**c**) OH, (**d**) MDA8 O$_3$, (**e**) PM$_{2.5}$, and (**f**) NO$_3^-$ in China, estimated as the differences between the Base and NoEm cases.

additional chlorine emissions, the particulate Cl$^-$ concentration increased significantly in inland China, with the largest increase in the Sichuan Basin (4.5 µg m^{-3}) and little change in west China. The increase is in the range of 1.5–3.5 µg m^{-3} in the North China Plain and <0.5 µg m^{-3} in south China.

The spatial distribution of ΔCl atoms is also consistent with that of the additional chlorine emissions and ΔCl$^-$, showing the largest increment in the Sichuan Basin (about 4.5–5 × 10^3 molec. cm^{-3}). There is also a moderate increase in Cl atoms in the Northeast Plain and North China Plain, with

a range of $1.5–4 \times 10^3$ molec. cm^{-3}. Only a minor increase in Cl atoms is found in south China ($< 1 \times 10^3$ molec. cm^{-3}).

As discussed earlier in Sect. 3.2, increased Cl atoms could lead to more HO_2 and OH via VOC oxidation. Combined with increased NO_x associated with the release of NO_2 upon the photolysis of $ClNO_2$, further increases in both O_3 and OH could also be expected. The increase in OH is around $2–9 \times 10^4$ molec. cm^{-3} in central and eastern China on an annual mean basis. The increase in MDA8 O_3 surface concentrations ranges from 0.5 to 3 ppbv in central and eastern China and reaches up to 3.5 ppbv in the Sichuan Basin on an annual average. The impacts of chlorine sources on O_3 formation also vary with seasons. Although O_3 pollution is generally severe in summer, the change in MDA8 O_3 due to the additional chlorine sources is relatively minor, with maxima of 0.7 ppbv in the Sichuan Basin and <0.5 ppbv in most other regions averaged in summer. In contrast, the increase is most obvious in winter, with a maximum of 5.2 ppbv in the Sichuan Basin seasonally on average.

The effects of the additional chlorine emissions on surface $PM_{2.5}$ concentrations are complicated. The North China Plain shows the largest increase (3–4.5 µg m^{-3} annually on average), mainly due to the increase in Cl$^-$, which could also promote the heterogeneous $N_2O_5 + Cl$ chemistry and lead to more NO_3^- production (C. Chen et al., 2021). In contrast, the Sichuan Basin exhibits both an increase (by up to 4.2 µg m^{-3}) and a decrease (by up to 3.7 µg m^{-3}). The decrease in $PM_{2.5}$ in the Sichuan Basin is mainly due to the large decrease in NO_3^- there. In the Sichuan Basin, nitrate formation is dominated by the heterogeneous hydrolysis of N_2O_5 (Tian et al., 2019), while the additional Cl$^-$ could hinder the path of N_2O_5 hydrolysis due to the competition with the path of $ClNO_2$ formation. Consequently, the additional chlorine emissions result in a decrease in NO_3^- of up to 5.6 µg m^{-3} in the Sichuan Basin annually on average.

In addition, NH_4^+ concentrations could also be affected through the Reaction (R5):

$$HCl(g) + NH_3(g) \rightarrow NH_4^+ + Cl^-. \tag{R5}$$
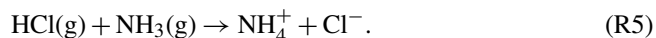
In the Northeast Plain and North China Plain where anthropogenic and biomass burning emissions of HCl are high, the annual mean NH_4^+ surface concentrations are increased by 0.5–1.5 µg m^{-3} (Fig. S11a). NH_4^+ concentrations are also affected by the gas–particle partitioning equilibrium and decrease as the pH value gets higher (or increase with H$^+$ concentrations). Therefore, the competition between the heterogeneous $N_2O_5 + Cl$ chemistry and N_2O_5 hydrolysis could also affect the formation of NH_4^+. In other words, increased Cl$^-$ concentrations could result in less H$^+$ and thus less NH_4^+. Consequently, there is also some decrease in NH_4^+ concentrations in the Sichuan Basin associated with the large decrease in NO_3^- concentrations. In contrast, little change is found for surface SO_4^{2-} concentrations, less than 0.5 µg m^{-3} in most regions of China (Fig. S11b).

It is worth mentioning that the effects of the additional chlorine emissions work mainly through the heterogeneous $N_2O_5 + Cl$ chemistry. Without this heterogeneous chemistry, the increase in chlorine emissions shows only a minor change in Cl atoms ($<10^3$ molec. cm^{-3} in China, estimated as the difference between the NoHet and NoEmHet cases in Fig. S12). The impact of chlorine emissions on O_3 concentrations also weakens when the heterogeneous $N_2O_5 + Cl$ chemistry is turned off, with an increase of 0.5–1 ppbv in MDA8 O_3 annually on average (vs. 0.5–3 ppbv mentioned above).

On the other hand, the impacts of heterogeneous $N_2O_5 + Cl$ chemistry on air quality in inland China would be seriously underestimated if the additional anthropogenic and biomass burning chlorine sources are ignored. If only sea salt chlorine emission is included in the simulation, the increase in $ClNO_2$ surface concentrations resulting from heterogeneous $N_2O_5 + Cl$ chemistry only occurs in coastal regions due to the heterogeneous uptake of N_2O_5 on sea salt chloride aerosols (by up to 260 pptv annually on average, indicated by the difference between the NoEm and NoEmHet cases, Fig. S13). Consequently, the increase in Cl atoms and MDA8 O_3 surface concentrations is found mainly in coastal regions. For instance, annual mean MDA8 O_3 concentrations are increased by up to 2 ppbv in coastal regions, but by less than 0.5 ppbv in inland China. In other words, the dominance of the heterogeneous $N_2O_5 + Cl$ chemistry in the impact of chlorine chemistry on air quality in China is to a large extent driven by the additional chlorine emissions.

3.4 The effect of heterogeneous $N_2O_5 + Cl$ chemistry in response to parameterizations for $\gamma_{N_2O_5}$ and φ_{ClNO_2}

It should be noted that the impact of the heterogeneous $N_2O_5 + Cl$ chemistry on air quality not only depends on the amount of chlorine emissions but is also sensitive to the parameterizations for $\gamma_{N_2O_5}$ and φ_{ClNO_2}. As discussed earlier (Fig. 3a), there exists a large difference in simulated N_2O_5 between the Base and NoEm cases at the Wangdu site, implying the sensitivity of $\gamma_{N_2O_5}$ to chlorine emissions in the Yu parameterization and thus the importance of non-sea-salt chlorine emissions in China. This is consistent with the dependence on chloride in the Yu parameterization, which is included to better reproduce $\gamma_{N_2O_5}$ observations in China (Yu et al., 2020). The comparison between the Base and NoHet cases ($\gamma_{N_2O_5} = 0.016$ and 0.014, respectively) also suggests that the heterogeneous uptake of N_2O_5 on chloride-containing aerosol surfaces in the Yu parameterization is an important loss pathway of N_2O_5 and should not be ignored.

Unlike the Yu parameterization, N_2O_5 concentrations have little dependence on chlorine emissions in the McDuffie parameterization (Fig. 3a). This insensitivity to chlorine emissions could be expected from Eq. (2), where the dependence on aerosol chloride is not included so as to better reproduce wintertime reactive nitrogen observations in the eastern US.
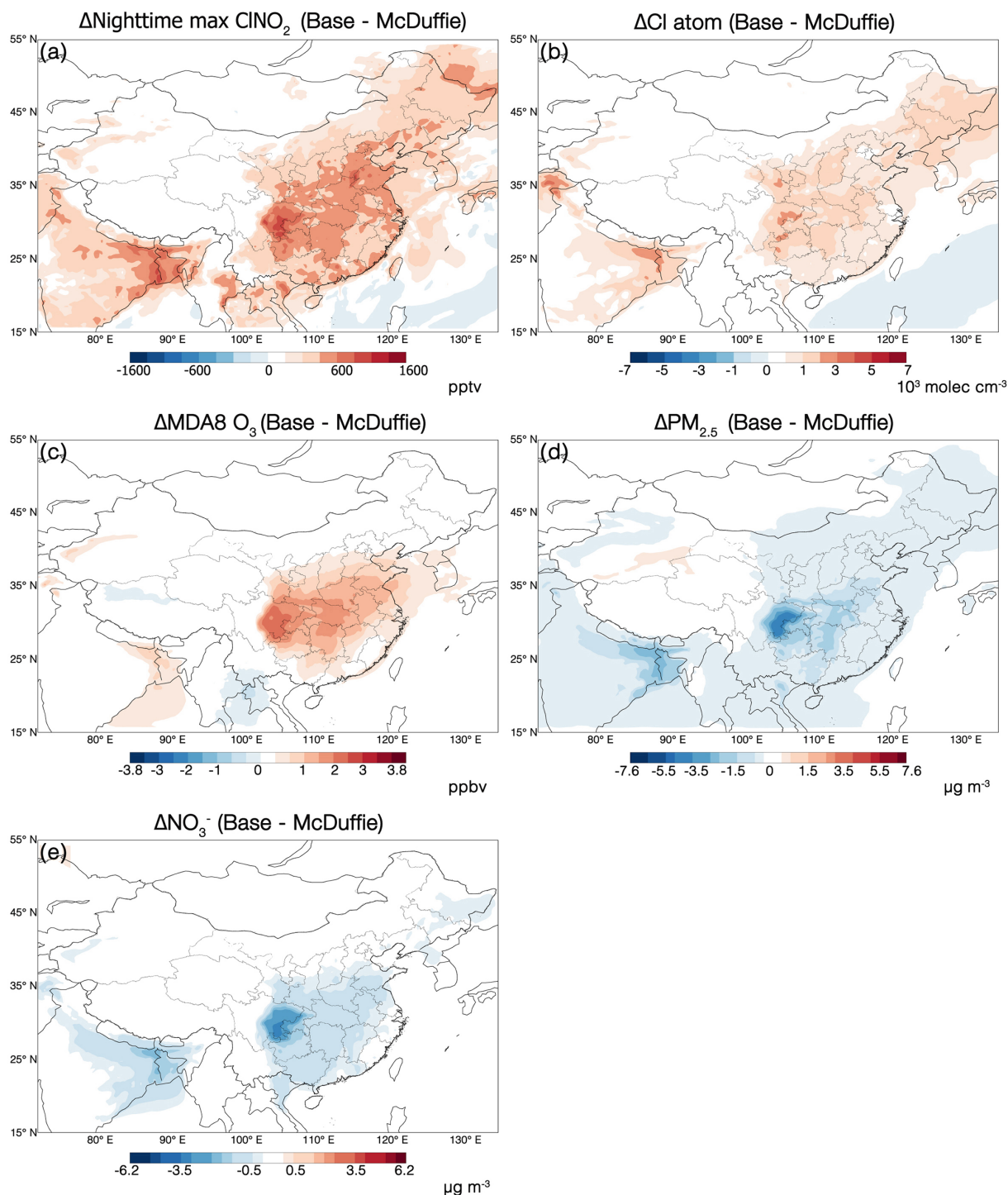
Figure 8. Effects of different parameterizations on annual mean surface concentrations of **(a)** nighttime max ClNO$_2$, **(b)** Cl atoms, **(c)** MDA8 O$_3$, **(d)** PM$_{2.5}$, and **(e)** NO$_3^-$ in China, estimated as the differences between the Base and McDuffie cases.

The little dependence of $\gamma_{N_2O_5}$ on concentrations of Cl$^-$ together with the lower value of φ_{ClNO_2} make the results from the McDuffie case less sensitive to chlorine emissions, producing fewer ClNO$_2$ and Cl atoms compared with the Base case (with the Yu parameterization), although with the same

emission. Consequently, the McDuffie case produces less O$_3$, with annual mean surface concentrations of MDA8 O$_3$ lower by 0.47 ppbv averaged in China (by up to 2 ppbv in the Sichuan Basin) but results in more PM$_{2.5}$ (0.63 µg m^{-3} averaged in China and up to 4.7 µg m^{-3} in the Sichuan Basin

on an annual mean basis mainly due to changes in NO_3^-) (Fig. 8). In other words, compared to the Base case with the Yu parameterization, the impacts of chlorine emissions on annual MDA8 O_3 and $PM_{2.5}$ in the McDuffie case have been decreased by 48 % and 27 %, respectively, averaged in China. Therefore, even with the same amounts of chlorine emissions, the impacts of the heterogeneous $N_2O_5 + Cl$ chemistry on air quality vary significantly with different parameterizations.

4   Conclusions

Considering the importance of chlorine chemistry in modulating the O_3 and $PM_{2.5}$ as well as the previously ignored chlorine emission from anthropogenic and biomass burning, we updated the GOES-Chem model in this study with comprehensive chlorine emissions and a new parameterization based on the study of Yu et al. (2020) for the heterogeneous $N_2O_5 + Cl$ chemistry, followed by the extensive evaluation of model performance. Through the utilization of a large number of observational datasets, we found a substantial improvement has been achieved by the additional chlorine emissions, with NMB decreasing from −96 % to −79 % to −36 % to 39 % for Cl^- simulation. The comparison with observed N_2O_5 and $ClNO_2$ also indicates better model performance with the Yu parameterization while $\gamma_{N_2O_5}$ and φ_{ClNO_2} are underestimated in the McDuffie parameterization (a default setting in GEOS-Chem), resulting in larger model bias. The simulation of O_3 and $PM_{2.5}$ also agrees better with observations in general in the Base case (with the additional chlorine emissions and the Yu parameterization) than the others.

Total tropospheric chlorine chemistry could increase Cl atoms by up to 7×10^3 molec. cm^{-3} and leads to an increase of up to 4.5 ppbv in MDA8 O_3 but a decrease of up to 7.9 µg m^{-3} in $PM_{2.5}$ concentrations on an annual mean basis in China. The decrease in $PM_{2.5}$ is mainly associated with the decrease in NO_3^- and NH_4^+, by up to 6.4 and 1.9 µg m^{-3}, respectively. The results also indicate that the heterogeneous $N_2O_5 + Cl$ chemistry dominates the impact of chlorine chemistry, accounting for 83 % and 90 % of total change in O_3 and $PM_{2.5}$ concentrations. In other words, the chlorine chemistry without the heterogeneous $N_2O_5 + Cl$ chemistry has a minor effect on annual mean MDA8 O_3 (less than 0.7 ppbv) and $PM_{2.5}$ (less than 1.5 µg m^{-3}) concentrations in China. This mechanism is particularly useful in elucidating the commonly seen O_3 underestimations relative to observations (e.g., Ma et al. 2019).

The effect of the heterogeneous $N_2O_5 + Cl$ chemistry is sensitive to chlorine emissions. With the additional anthropogenic and biomass burning sources, simulated $PM_{2.5}$ concentrations are increased by up to 4.5 µg m^{-3} in the North China Plain but decreased by up to 3.7 µg m^{-3} in the Sichuan Basin on an annual basis. The latter is mainly driven by

the decrease in NO_3^- due to the competition between the formation of $ClNO_2$ and HNO_3 upon the uptake of N_2O_5 on aerosol surfaces. The additional emissions also increase Cl atoms and OH in China associated with the photolysis of $ClNO_2$, consequently leading to an increase in annual mean MDA8 O_3 concentrations by up to 3.5 ppbv. In contrast, the significance of the heterogeneous $N_2O_5 + Cl$ chemistry, especially over inland China, would be severely underestimated if only sea salt chlorine is considered, with only a slight increase in MDA8 O_3 (<0.5 ppbv) and a minor decrease in $PM_{2.5}$ (< 1.5 µg m^{-3}) in inland China.

Moreover, we found the importance of chlorine chemistry not only depends on the amount of emissions, but is also sensitive to the parameterizations for the heterogeneous $N_2O_5 + Cl$ chemistry. Although they have the same emission, the effects on MDA8 O_3 and $PM_{2.5}$ in China from the McDuffie case are lower compared to the results with the Yu parameterization: differing by 48 % and 27 % in the annual average, respectively.

Author contributions. QW designed the study. XY performed the analysis. NM, WH, and BY provided the observation data. ZH and JZ provided the emission inventory. NM, WH, YG, BY, NY, JT, JH, YC, and HS discussed the results. XY and QW wrote the paper with input from all the other co-authors.

References

Anttila, T., Kiendler-Scharr, A., Tillmann, R., and Mentel, T. F.: On the Reactive Uptake of Gaseous Compounds by Organic-Coated Aqueous Aerosols: Theoretical Analysis and Application to the Heterogeneous Hydrolysis of N$_2$O$_5$, J. Phys. Chem. A, 110, 10435–10443, https://doi.org/10.1021/jp062403c, 2006..

Atkinson, R., Baulch, D. L., Cox, R. A., Crowley, J. N., Hampson, R. F., Hynes, R. G., Jenkin, M. E., Rossi, M. J., Troe, J., and IUPAC Subcommittee: Evaluated kinetic and photochemical data for atmospheric chemistry: Volume II – gas phase reactions of organic species, Atmos. Chem. Phys., 6, 3625–4055, https://doi.org/10.5194/acp-6-3625-2006, 2006.

Bertram, T. H. and Thornton, J. A.: Toward a general parameterization of N$_2$O$_5$ reactivity on aqueous particles: the competing effects of particle liquid water, nitrate and chloride, Atmos. Chem. Phys., 9, 8351–8363, https://doi.org/10.5194/acp-9-8351-2009, 2009.

Bertram, T. H., Perring, A. E., Wooldridge, P. J., Dibb, J., Avery, M. A., and Cohen, R. C.: On the export of reactive nitrogen from Asia: NO$_x$ partitioning and effects on ozone, Atmos. Chem. Phys., 13, 4617–4630, https://doi.org/10.5194/acp-13-4617-2013, 2013.

Chang, W. L., Brown, S. S., Stutz, J., Middlebrook, A. M., Bahreini, R., Wagner, N. L., Dubé, W. P., Pollack, I. B., Ryerson, T. B., and Riemer, N.: Evaluating N$_2$O$_5$ heterogeneous hydrolysis parameterizations for CalNex 2010, J. Geophys. Res.-Atmos., 121, 5051–5070, https://doi.org/10.1002/2015JD024737, 2016.

Chen, C., Zhang, H., Yan, W., Wu, N., Zhang, Q., and He, K.: Aerosol water content enhancement leads to changes in the major formation mechanisms of nitrate and secondary organic aerosols in winter over the North China Plain, Environ. Pollut., 287, 117625, https://doi.org/10.1016/j.envpol.2021.117625, 2021.

Chen, W., Ye, Y., Hu, W., Zhou, H., Pan, T., Wang, Y., Song, W., Song, Q., Ye, C., Wang, C., Wang, B., Huang, S., Yuan, B., Zhu, M., Lian, X., Zhang, G., Bi, X., Jiang, F., Liu, J., Canonaco, F., Prevot, A. S. H., Shao, M., and Wang, X.: Real-Time Characterization of Aerosol Compositions, Sources, and Aging Processes in Guangzhou During PRIDE-GBA 2018 Campaign, J. Geophys. Res.-Atmos., 126, e2021JD035114, https://doi.org/10.1029/2021JD035114, 2021.

Choi, M. S., Qiu, X., Zhang, J., Wang, S., Li, X., Sun, Y., Chen, J., and Ying, Q.: Study of Secondary Organic Aerosol Formation from Chlorine Radical-Initiated Oxidation of Volatile Organic Compounds in a Polluted Atmosphere Using a 3D Chemical Transport Model, Environ. Sci. Technol., 54, 13409–13418, https://doi.org/10.1021/acs.est.0c02958, 2020.

Dai, J., Liu, Y., Wang, P., Fu, X., Xia, M., and Wang, T.: The impact of sea-salt chloride on ozone through heterogeneous reaction with N$_2$O$_5$ in a coastal region of south China, Atmos. Environ.,

236, 117604, https://doi.org/10.1016/j.atmosenv.2020.117604, 2020.

DeCarlo, P. F., Kimmel, J. R., Trimborn, A., Northway, M. J., Jayne, J. T., Aiken, A. C., Gonin, M., Fuhrer, K., Horvath, T., Docherty, K. S., Worsnop, D. R., and Jimenez, J. L.: Field-Deployable, High-Resolution, Time-of-Flight Aerosol Mass Spectrometer, Anal. Chem., 78, 8281–8289, https://doi.org/10.1021/ac061249n, 2006.

Finlayson-Pitts, B. J., Ezell, M. J., and Pitts, J. N. J.: Formation of chemically active chlorine compounds by reactions of atmospheric NaCl particles with gaseous N$_2$O$_5$ and ClONO$_2$, Cheminform, 20, 241–244, 1989.

Fountoukis, C. and Nenes, A.: ISORROPIA II: a computationally efficient thermodynamic equilibrium model for K$^+$–Ca^{2+}–Mg^{2+}–NH$_4^+$–Na$^+$–SO$_4^{2-}$–NO$_3^-$–Cl$^-$–H$_2$O aerosols, Atmos. Chem. Phys., 7, 4639–4659, https://doi.org/10.5194/acp-7-4639-2007, 2007.

Fu, X., Wang, T., Wang, S., Zhang, L., Cai, S., Xing, J., and Hao, J.: Anthropogenic Emissions of Hydrogen Chloride and Fine Particulate Chloride in China, Environ. Sci. Technol., 52, 1644–1654, https://doi.org/10.1021/acs.est.7b05030, 2018.

Geng, G., Zhang, Q., Martin, R. V., Van Donkelaar, A., Huo, H., Che, H., Lin, J., and He, K.: Estimating long-term PM$_{2.5}$ concentrations in China using satellite-based aerosol optical depth and a chemical transport model, Remote Sens. Environ., 166, 262–270, 2015.

Griffiths, P. T., Badger, C. L., Cox, R. A., Folkers, M., Henk, H. H., and Mentel, T. F.: Reactive Uptake of N$_2$O$_5$ by Aerosols Containing Dicarboxylic Acids. Effect of Particle Phase, Composition, and Nitrate Content, J. Phys. Chem. A, 113, 5082–5090, https://doi.org/10.1021/jp8096814, 2009.

Gross, S., Iannone, R., Xiao, S., and Bertram, A. K.: Reactive uptake studies of NO$_3$ and N$_2$O$_5$ on alkenoic acid, alkanoate, and polyalcohol substrates to probe nighttime aerosol chemistry, Phys. Chem. Chem. Phys., 11, 7792–7803, https://doi.org/10.1039/B904741G, 2009.

Guenther, A., Karl, T., Harley, P., Wiedinmyer, C., Palmer, P. I., and Geron, C.: Estimates of global terrestrial isoprene emissions using MEGAN (Model of Emissions of Gases and Aerosols from Nature), Atmos. Chem. Phys., 6, 3181–3210, https://doi.org/10.5194/acp-6-3181-2006, 2006.

Haskins, J. D., Lee, B. H., Lopez-Hilifiker, F. D., Peng, Q., Jaeglé, L., Reeves, J. M., Schroder, J. C., Campuzano-Jost, P., Fibiger, D., McDuffie, E. E., Jiménez, J. L., Brown, S. S., and Thornton, J. A.: Observational Constraints on the Formation of Cl$_2$ From the Reactive Uptake of ClNO$_2$ on Aerosols in the Polluted Marine Boundary Layer, J. Geophys. Res.-Atmos., 124, 8851–8869, https://doi.org/10.1029/2019JD030627, 2019.

Hong, Y., Liu, Y., Chen, X., Fan, Q., Chen, C., Chen, X., and Wang, M.: The role of anthropogenic chlorine emission in surface ozone formation during different seasons over eastern China, Sci. Total Environ., 723, 137697, https://doi.org/10.1016/j.scitotenv.2020.137697, 2020.

Hossaini, R., Chipperfield, M. P., Saiz-Lopez, A., Fernandez, R., Monks, S., Feng, W., Brauer, P., and von Glasow, R.: A global model of tropospheric chlorine chemistry: Organic versus inorganic sources and impact on methane oxidation, J. Geophys. Res.-Atmos., 121, 14,271-214,297, https://doi.org/10.1002/2016JD025756, 2016.

Huang, Z., Zhong, Z., Sha, Q., Xu, Y., Zhang, Z., Wu, L., Wang, Y., Zhang, L., Cui, X., Tang, M., Shi, B., Zheng, C., Li, Z., Hu, M., Bi, L., Zheng, J., and Yan, M.: An updated model-ready emission inventory for Guangdong Province by incorporating big data and mapping onto multiple chemical mechanisms, Sci. Total Environ., 769, 144535, https://doi.org/10.1016/j.scitotenv.2020.144535, 2021.

Jaeglé, L., Quinn, P. K., Bates, T. S., Alexander, B., and Lin, J.-T.: Global distribution of sea salt aerosols: new constraints from in situ and remote sensing observations, Atmos. Chem. Phys., 11, 3137–3157, https://doi.org/10.5194/acp-11-3137-2011, 2011.

Kercher, J. P., Riedel, T. P., and Thornton, J. A.: Chlorine activation by N$_2$O$_5$: simultaneous, in situ detection of ClNO$_2$ and N$_2$O$_5$ by chemical ionization mass spectrometry, Atmos. Meas. Tech., 2, 193–204, https://doi.org/10.5194/amt-2-193-2009, 2009.

Lawler, M. J., Sander, R., Carpenter, L. J., Lee, J. D., von Glasow, R., Sommariva, R., and Saltzman, E. S.: HOCl and Cl$_2$ observations in marine air, Atmos. Chem. Phys., 11, 7617–7628, https://doi.org/10.5194/acp-11-7617-2011, 2011.

Le Breton, M., Hallquist, Å. M., Pathak, R. K., Simpson, D., Wang, Y., Johansson, J., Zheng, J., Yang, Y., Shang, D., Wang, H., Liu, Q., Chan, C., Wang, T., Bannan, T. J., Priestley, M., Percival, C. J., Shallcross, D. E., Lu, K., Guo, S., Hu, M., and Hallquist, M.: Chlorine oxidation of VOCs at a semi-rural site in Beijing: significant chlorine liberation from ClNO$_2$ and subsequent gas- and particle-phase Cl–VOC production, Atmos. Chem. Phys., 18, 13013–13030, https://doi.org/10.5194/acp-18-13013-2018, 2018.

Li, G., Su, H., Ma, N., Tao, J., Kuang, Y., Wang, Q., Hong, J., Zhang, Y., Kuhn, U., Zhang, S., Pan, X., Lu, N., Tang, M., Zheng, G., Wang, Z., Gao, Y., Cheng, P., Xu, W., Zhou, G., Zhao, C., Yuan, B., Shao, M., Ding, A., Zhang, Q., Fu, P., Sun, Y., Pöschl, U., and Cheng, Y.: Multiphase chemistry experiment in Fogs and Aerosols in the North China Plain (McFAN): integrated analysis and intensive winter campaign 2018, Faraday Discuss., 226, 207–222, https://doi.org/10.1039/D0FD00099J, 2021.

Li, K., Jacob, D. J., Liao, H., Shen, L., Zhang, Q., and Bates, K. H.: Anthropogenic drivers of 2013–2017 trends in summer surface ozone in China, P. Natl. Acad. Sci. USA, 116, 422–427, https://doi.org/10.1073/pnas.1812168116, 2019.

Li, M., Zhang, Q., Kurokawa, J.-I., Woo, J.-H., He, K., Lu, Z., Ohara, T., Song, Y., Streets, D. G., Carmichael, G. R., Cheng, Y., Hong, C., Huo, H., Jiang, X., Kang, S., Liu, F., Su, H., and Zheng, B.: MIX: a mosaic Asian anthropogenic emission inventory under the international collaboration framework of the MICS-Asia and HTAP, Atmos. Chem. Phys., 17, 935–963, https://doi.org/10.5194/acp-17-935-2017, 2017.

Li, Q., Zhang, L., Wang, T., Tham, Y. J., Ahmadov, R., Xue, L., Zhang, Q., and Zheng, J.: Impacts of heterogeneous uptake of dinitrogen pentoxide and chlorine activation on ozone and reactive nitrogen partitioning: improvement and application of the WRF-Chem model in southern China, Atmos. Chem. Phys., 16, 14875–14890, https://doi.org/10.5194/acp-16-14875-2016, 2016.

Liu, X., Qu, H., Huey, L. G., Wang, Y., Sjostedt, S., Zeng, L., Lu, K., Wu, Y., Hu, M., Shao, M., Zhu, T., and Zhang, Y.: High Levels of Daytime Molecular Chlorine and Nitryl Chloride at a Rural Site on the North China Plain, Environ. Sci. Technol., 51, 9588–9595, https://doi.org/10.1021/acs.est.7b03039, 2017.

Liu, Y., Fan, Q., Chen, X., Zhao, J., Ling, Z., Hong, Y., Li, W., Chen, X., Wang, M., and Wei, X.: Modeling the impact of chlorine emissions from coal combustion and prescribed waste incineration on tropospheric ozone formation in China, Atmos. Chem. Phys., 18, 2709–2724, https://doi.org/10.5194/acp-18-2709-2018, 2018.

Lobert, J. M., Keene, W. C., Logan, J. A., and Yevich, R.: Global chlorine emissions from biomass burning: Reactive Chlorine Emissions Inventory, J. Geophys. Res.-Atmos., 104, 8373–8389, https://doi.org/10.1029/1998JD100077, 1999.

Ma, M., Gao, Y., Wang, Y., Zhang, S., Leung, L. R., Liu, C., Wang, S., Zhao, B., Chang, X., Su, H., Zhang, T., Sheng, L., Yao, X., and Gao, H.: Substantial ozone enhancement over the North China Plain from increased biogenic emissions due to heat waves and land cover in summer 2017, Atmos. Chem. Phys., 19, 12195–12207, https://doi.org/10.5194/acp-19-12195-2019, 2019.

McDuffie, E. E., Fibiger, D. L., Dubé, W. P., Lopez Hilfiker, F., Lee, B. H., Jaeglé, L., Guo, H., Weber, R. J., Reeves, J. M., Weinheimer, A. J., Schroder, J. C., Campuzano-Jost, P., Jimenez, J. L., Dibb, J. E., Veres, P., Ebben, C., Sparks, T. L., Wooldridge, P. J., Cohen, R. C., Campos, T., Hall, S. R., Ullmann, K., Roberts, J. M., Thornton, J. A., and Brown, S. S.: ClNO$_2$ Yields From Aircraft Measurements During the 2015 WINTER Campaign and Critical Evaluation of the Current Parameterization, J. Geophys. Res.-Atmos., 123, 12,994-913,015, https://doi.org/10.1029/2018JD029358, 2018a.

McDuffie, E. E., Fibiger, D. L., Dubé, W. P., Lopez-Hilfiker, F., Lee, B. H., Thornton, J. A., Shah, V., Jaeglé, L., Guo, H., Weber, R. J., Michael Reeves, J., Weinheimer, A. J., Schroder, J. C., Campuzano-Jost, P., Jimenez, J. L., Dibb, J. E., Veres, P., Ebben, C., Sparks, T. L., Wooldridge, P. J., Cohen, R. C., Hornbrook, R. S., Apel, E. C., Campos, T., Hall, S. R., Ullmann, K., and Brown, S. S.: Heterogeneous N$_2$O$_5$ Uptake During Winter: Aircraft Measurements During the 2015 WINTER Campaign and Critical Evaluation of Current Parameterizations, J. Geophys. Res.-Atmos., 123, 4345–4372, https://doi.org/10.1002/2018JD028336, 2018b.

Mitroo, D., Gill, T. E., Haas, S., Pratt, K. A., and Gaston, C. J.: ClNO$_2$ Production from N$_2$O$_5$ Uptake on Saline Playa Dusts: New Insights into Potential Inland Sources of ClNO$_2$, Environ. Sci. Technol., 53, 7442–7452, 2019.

Morgan, W. T., Ouyang, B., Allan, J. D., Aruffo, E., Di Carlo, P., Kennedy, O. J., Lowe, D., Flynn, M. J., Rosenberg, P. D., Williams, P. I., Jones, R., McFiggans, G. B., and Coe, H.: Influence of aerosol chemical composition on N$_2$O$_5$ uptake: airborne regional measurements in northwestern Europe, Atmos. Chem. Phys., 15, 973–990, https://doi.org/10.5194/acp-15-973-2015, 2015.

Ng, N. L., Herndon, S. C., Trimborn, A., Canagaratna, M. R., Croteau, P. L., Onasch, T. B., Sueper, D., Worsnop, D. R., Zhang, Q., Sun, Y. L., and Jayne, J. T.: An Aerosol Chemical Speciation Monitor (ACSM) for Routine Monitoring of the Composition and Mass Concentrations of Ambient Aerosol, Aerosol Sci. Technol., 45, 780–794, https://doi.org/10.1080/02786826.2011.560211, 2011.

Osthoff, H. D., Roberts, J. M., Ravishankara, A. R., Williams, E. J., Lerner, B. M., Sommariva, R., Bates, T. S., Coffman, D., Quinn, P. K., Dibb, J. E., Stark, H., Burkholder, J. B., Talukdar, R. K., Meagher, J., Fehsenfeld, F. C., and Brown, S. S.: High levels

of nitryl chloride in the polluted subtropical marine boundary layer, Nat. Geosci., 1, 324–328, https://doi.org/10.1038/ngeo177, 2008.

Riedel, T. P., Bertram, T. H., Crisp, T. A., Williams, E. J., Lerner, B. M., Vlasenko, A., Li, S. M., Gilman, J., De Gouw, J., and Bon, D. M.: Nitryl Chloride and Molecular Chlorine in the Coastal Marine Boundary Layer, Environ. Sci. Technol., 46, 10463–10470, 2012.

Riedel, T. P., Wolfe, G. M., Danas, K. T., Gilman, J. B., Kuster, W. C., Bon, D. M., Vlasenko, A., Li, S. M., Williams, E. J., Lerner, B. M., Veres, P. R., Roberts, J. M., Holloway, J. S., Lefer, B., Brown, S. S., and Thornton, J. A.: An MCM modeling study of nitryl chloride (ClNO$_2$) impacts on oxidation, ozone production and nitrogen oxide partitioning in polluted continental outflow, Atmos. Chem. Phys., 14, 3789–3800, https://doi.org/10.5194/acp-14-3789-2014, 2014.

Riemer, N., Vogel, H., Vogel, B., Anttila, T., Kiendler-Scharr, A., and Mentel, T. F.: Relative importance of organic coatings for the heterogeneous hydrolysis of N$_2$O$_5$ during summer in Europe, J. Geophys. Res.-Atmos., 114, D17307, https://doi.org/10.1029/2008JD011369, 2009.

Saiz-Lopez, A. and von Glasow, R.: Reactive halogen chemistry in the troposphere, Chem. Soc. Rev., 41, 6448–6472, https://doi.org/10.1039/C2CS35208G, 2012.

Sarwar, G., Simon, H., Xing, J., and Mathur, R.: Importance of tropospheric ClNO$_2$ chemistry across the Northern Hemisphere, Geophys. Res. Lett., 41, 4050–4058, https://doi.org/10.1002/2014GL059962, 2014.

Schmidt, J. A., Jacob, D. J., Horowitz, H. M., Hu, L., Sherwen, T., Evans, M. J., Liang, Q., Suleiman, R. M., Oram, D. E., Le Breton, M., Percival, C. J., Wang, S., Dix, B., and Volkamer, R.: Modeling the observed tropospheric BrO background: Importance of multiphase chemistry and implications for ozone, OH, and mercury, J. Geophys. Res.-Atmos., 121, 11,819-811,835, https://doi.org/10.1002/2015JD024229, 2016.

Sherwen, T., Schmidt, J. A., Evans, M. J., Carpenter, L. J., Großmann, K., Eastham, S. D., Jacob, D. J., Dix, B., Koenig, T. K., Sinreich, R., Ortega, I., Volkamer, R., Saiz-Lopez, A., Prados-Roman, C., Mahajan, A. S., and Ordóñez, C.: Global impacts of tropospheric halogens (Cl, Br, I) on oxidants and composition in GEOS-Chem, Atmos. Chem. Phys., 16, 12239–12271, https://doi.org/10.5194/acp-16-12239-2016, 2016.

Sherwen, T., Evans, M. J., Sommariva, R., Hollis, L. D. J., Ball, S. M., Monks, P. S., Reed, C., Carpenter, L. J., Lee, J. D., Forster, G., Bandy, B., Reeves, C. E., and Bloss, W. J.: Effects of halogens on European air-quality, Faraday Discuss., 200, 75–100, https://doi.org/10.1039/C7FD00026J, 2017.

Simmonds, P. G., Manning, A. J., Cunnold, D. M., McCulloch, A., O'Doherty, S., Derwent, R. G., Krummel, P. B., Fraser, P. J., Dunse, B., Porter, L. W., Wang, R. H. J., Greally, B. R., Miller, B. R., Salameh, P., Weiss, R. F., and Prinn, R. G.: Global trends, seasonal cycles, and European emissions of dichloromethane, trichloroethene, and tetrachloroethene from the AGAGE observations at Mace Head, Ireland, and Cape Grim, Tasmania, J. Geophys. Res.-Atmos., 111, D18304, https://doi.org/10.1029/2006JD007082, 2006.

Simpson, W. R., Brown, S. S., Saiz-Lopez, A., Thornton, J. A., and von Glasow, R.: Tropospheric Halogen Chemistry: Sources, Cycling, and Impacts, Chem. Rev., 115, 4035–4062, https://doi.org/10.1021/cr5006638, 2015.

Staudt, S., Gord, J. R., Karimova, N. V., McDuffie, E. E., Brown, S. S., Gerber, R. B., Nathanson, G. M., and Bertram, T. H.: Sulfate and Carboxylate Suppress the Formation of ClNO$_2$ at Atmospheric Interfaces, ACS Earth and Space Chemistry, 3, 1987–1997, https://doi.org/10.1021/acsearthspacechem.9b00177, 2019.

Thornton, J. A., Braban, C. F., and Abbatt, J. P. D.: N$_2$O$_5$ hydrolysis on sub-micron organic aerosols: the effect of relative humidity, particle phase, and particle size, Phys. Chem. Chem. Phys., 5, 4593–4603, https://doi.org/10.1039/B307498F, 2003.

Tian, M., Liu, Y., Yang, F., Zhang, L., Peng, C., Chen, Y., Shi, G., Wang, H., Luo, B., Jiang, C., Li, B., Takeda, N., and Koizumi, K.: Increasing importance of nitrate formation for heavy aerosol pollution in two megacities in Sichuan Basin, southwest China, Environ. Pollut., 250, 898–905, https://doi.org/10.1016/j.envpol.2019.04.098, 2019.

van der Werf, G. R., Randerson, J. T., Giglio, L., Collatz, G. J., Mu, M., Kasibhatla, P. S., Morton, D. C., DeFries, R. S., Jin, Y., and van Leeuwen, T. T.: Global fire emissions and the contribution of deforestation, savanna, forest, agricultural, and peat fires (1997–2009), Atmos. Chem. Phys., 10, 11707–11735, https://doi.org/10.5194/acp-10-11707-2010, 2010.

Wang, S., Su, H., Chen, C., Tao, W., Streets, D. G., Lu, Z., Zheng, B., Carmichael, G. R., Lelieveld, J., Pöschl, U., and Cheng, Y.: Natural gas shortages during the "coal-to-gas" transition in China have caused a large redistribution of air pollution in winter 2017, P. Natl. Acad. Sci. USA, 117, 31018–31025, https://doi.org/10.1073/pnas.2007513117, 2020.

Wang, X., Jacob, D. J., Eastham, S. D., Sulprizio, M. P., Zhu, L., Chen, Q., Alexander, B., Sherwen, T., Evans, M. J., Lee, B. H., Haskins, J. D., Lopez-Hilfiker, F. D., Thornton, J. A., Huey, G. L., and Liao, H.: The role of chlorine in global tropospheric chemistry, Atmos. Chem. Phys., 19, 3981–4003, https://doi.org/10.5194/acp-19-3981-2019, 2019.

Wang, X., Jacob, D. J., Fu, X., Wang, T., and Liao, H.: Effects of Anthropogenic Chlorine on PM$_{2.5}$ and Ozone Air Quality in China, Environ. Sci. Technol., 54, 9908–9916, 2020.

Wang, Y., Shen, L., Wu, S., Mickley, L., He, J., and Hao, J.: Sensitivity of surface ozone over China to 2000–2050 global changes of climate and emissions, Atmos. Environ., 75, 374–382, 2013.

Xia, M., Wang, W., Wang, Z., Gao, J., Li, H., Liang, Y., Yu, C., Zhang, Y., Wang, P., Zhang, Y., Bi, F., Cheng, X., and Wang, T.: Heterogeneous Uptake of N$_2$O$_5$ in Sand Dust and Urban Aerosols Observed during the Dry Season in Beijing, Atmosphere, 10, 204, https://doi.org/10.3390/atmos10040204, 2019.

Xu, Z., Liu, M., Zhang, M., Song, Y., Wang, S., Zhang, L., Xu, T., Wang, T., Yan, C., Zhou, T., Sun, Y., Pan, Y., Hu, M., Zheng, M., and Zhu, T.: High efficiency of livestock ammonia emission controls in alleviating particulate nitrate during a severe winter haze episode in northern China, Atmos. Chem. Phys., 19, 5605–5613, https://doi.org/10.5194/acp-19-5605-2019, 2019.

Yang, X., Wang, T., Xia, M., Gao, X., Li, Q., Zhang, N., Gao, Y., Lee, S., Wang, X., Xue, L., Yang, L., and Wang, W.: Abundance and origin of fine particulate chloride in continental China, Sci. Total Environ., 624, 1041–1051, https://doi.org/10.1016/j.scitotenv.2017.12.205, 2018.

Yang, X., Wang, Q., Ma, N., Hu, W., Gao, Y., Huang, Z., Zheng, J., Yuan, B., Yang, N., Tao, J., Hong, J., Cheng, Y., and Su, H.: The impact of chlorine chemistry combined with heterogeneous N$_2$O$_5$ reactions on air quality in China, Zenodo [data set], https://doi.org/10.5281/zenodo.5957287, 2021.

Ye, C., Yuan, B., Lin, Y., Wang, Z., Hu, W., Li, T., Chen, W., Wu, C., Wang, C., Huang, S., Qi, J., Wang, B., Wang, C., Song, W., Wang, X., Zheng, E., Krechmer, J. E., Ye, P., Zhang, Z., Wang, X., Worsnop, D. R., and Shao, M.: Chemical characterization of oxygenated organic compounds in the gas phase and particle phase using iodide CIMS with FIGAERO in urban air, Atmos. Chem. Phys., 21, 8455–8478, https://doi.org/10.5194/acp-21-8455-2021, 2021.

Yu, C., Wang, Z., Xia, M., Fu, X., Wang, W., Tham, Y. J., Chen, T., Zheng, P., Li, H., Shan, Y., Wang, X., Xue, L., Zhou, Y., Yue, D., Ou, Y., Gao, J., Lu, K., Brown, S. S., Zhang, Y., and Wang, T.: Heterogeneous N$_2$O$_5$ reactions on atmospheric aerosols at four Chinese sites: improving model representation of uptake parameters, Atmos. Chem. Phys., 20, 4367–4378, https://doi.org/10.5194/acp-20-4367-2020, 2020.

Zhang, T., de Jong, M. C., Wooster, M. J., Xu, W., and Wang, L.: Trends in eastern China agricultural fire emissions derived from a combination of geostationary (Himawari) and polar (VIIRS) orbiter fire radiative power products, Atmos. Chem. Phys., 20, 10687–10705, https://doi.org/10.5194/acp-20-10687-2020, 2020.